

# Application of Disease System Analysis to Osteoporosis: From Temporal to Spatio-Temporal Assessment of Disease Progression and Intervention

Silvia Trichilo and Peter Pivonka

**Abstract** Osteoporosis (OP) is a progressive bone disorder regarded as an important worldwide health issue. OP is characterised by a slow reduction of the bone matrix and changes in the bone matrix properties. Novel drug treatments are continuously developed to reduce the risk of bone fractures. Assessing the effects of novel and existing treatments on OP can be challenging. This is due to the difficulties of establishing the effects of the drug on the disease progression as reflected in the slowly changing bone mineral density (BMD). In recent years, our understanding of the pathophysiology of OP has considerably improved. Biomarkers reflecting bone physiology have been identified at the cellular, tissue and organ levels. Cellular biomarkers reflect the dynamics of bone remodelling (i.e., bone formation and resorption) on a short time scale. On the other hand, tissue and organ scale biomarkers show changes of BMD and bone structural arrangements on a larger time scale. Biomarkers can be used to characterise bone remodelling and to quantify the effect of the drug on OP. Recently, the concept of disease system analysis (DSA) has been proposed as a novel approach to quantitatively characterise drug effects on disease progression. This approach integrates physiology, disease progression and drug treatment in a comprehensive mechanism-based modelling framework using a large amount of complementary biomarker data. This chapter will provide an overview of the use of DSA to characterise drug effects on OP. We will review classical (i.e., non-mechanistic) pharmacokinetic-pharmacodynamic (PK/PD) models used to study *drug dose-effect* responses. Latest mechanistic bone remodelling models will be presented together with the study of the effect of the drug denosumab on

---

S. Trichilo · P. Pivonka (✉)

St Vincent's Department of Surgery, The University of Melbourne,  
Melbourne, VIC, Australia  
e-mail: peter.pivonka@qut.edu.au

S. Trichilo · P. Pivonka

Australian Institute of Musculoskeletal Science, Melbourne, VIC, Australia  
e-mail: strichilo@student.unimelb.edu.au

P. Pivonka

School of Chemistry, Physics and Mechanical Engineering, Queensland University  
of Technology, Brisbane, QLD, Australia

© CISM International Centre for Mechanical Sciences 2018

P. Pivonka (ed.), *Multiscale Mechanobiology of Bone Remodeling  
and Adaptation*, CISM International Centre for Mechanical Sciences 578,  
DOI 10.1007/978-3-319-58845-2\_2

disease progression in postmenopausal osteoporosis (PMO). Finally, we will provide an outlook on how to extend the temporal mechanistic model towards a spatio-temporal description. We conclude that the development of fully mechanistic disease system models of OP has great potential to adequately predict the long-term effects of drug treatments on clinical outcomes. This may provide a means for patient-specific estimation of bone fracture risk.

## 1 Introduction

The objective of this chapter is to introduce the theoretical framework of disease system analysis (DSA) to analyse disease progression and therapeutic intervention in osteoporosis (OP). Firstly, we will introduce the classical pharmacokinetic (PK), pharmacodynamic (PD) and pharmacokinetic-pharmacodynamic (PK/PD) modelling approaches in the context of OP and drug interventions. The PK/PD framework will then be expanded towards DSA allowing for the classification of disease status and progression, together with assessment of various drug interventions. Two types of models will be discussed: (i) the one treating the symptoms of a disease and their response to the treatment directly, i.e., without consideration of the underlying biological system; (ii) the one treating the disease progression as a turnover model allowing the distinction between the disease progress and the effects of the drug on the disease status. Based on the limitations of current DSA models of OP, we introduce a comprehensive mechanism-based disease progression model. Key variables in this model are: bone cells concentrations (active osteoblasts, active osteoclasts and their precursor cells); cell-cell signalling pathway (RANK-RANKL-OPG pathway); hormonal (PTH) and local (TGF- $\beta$ ) regulatory factors; mechanical strains both at the macroscopic level of cortical and trabecular bone and at the microscopic level of the extra-vascular bone matrix. The latter variable provides the ability to account for the biomechanical feedback coming from osteocytes. Subsequently, this model is used to investigate postmenopausal osteoporosis (PMO) and its treatment with the anti-catabolic drug denosumab. Finally, we will provide an outlook on how to extend temporal models of bone remodelling to spatio-temporal models, a necessary prerequisite to accurately estimate the risk of bone fracture.

OP is a progressive disease characterised by fractures of spine, hip and wrist as primary clinical manifestations. It is a major health problem in the society placed alongside diseases such as breast cancer, cardiovascular diseases and diabetes mellitus when considering prevalence, lifetime risk and socio-economical impact [76, 143]. Most often, OP is diagnosed only after a fracture occurs, it is therefore referred to as *silent disease*. Because of its importance, many researchers are currently studying to understand the origin of the disease and to find effective treatments [13]. New drugs are continually being developed and trialled on animals, only the most promising ones are then tested on humans. Drug efficacy and safety are usually assessed using biomarkers. In general, biomarkers can be divided into two categories: *site-specific* and *non-site specific*. The former category allows to assess bone mineral density

(BMD) and bone quality at a particular bone site using X-ray imaging technologies. The latter category, also referred to as bone turnover markers (BTMs), allows to assess the activity of bone cells in the entire body by measuring bone molecular product concentrations in blood and/or urine [23].

Several scientific communities have approached the problem of OP aiming to better understand the deterioration of bone mechanical properties, to predict bone fracture risk and to quantify the effects of drugs on disease progression. The approach taken by materials, structural mechanics and biomedical engineering researchers is based on the development of deterministic methods including experimental testing techniques (e.g., mechanical characterisation and imaging-based methods) and computational models assessing bone mechanical behaviour at different scales [177].

On the other hand, the approach taken by clinical researchers investigating drug efficacy and safety is mainly based on the use of statistical methods, including randomised controlled trials (RCTs) [91]. The development of new drug treatments, however, is challenging. The trials require a large cohort of patients, due to the necessity of establishing a statistically significant anti-fracture benefit, and are long in duration, due to the slow progression of the disease.

Finally, basic bone scientists are concerned with the development of animal models (including genetically engineered animals) in order to investigate intra- and inter-cellular aspects of bone diseases and interventions [71]. This approach has significantly improved the knowledge of the bone physiology and the underlying mechanisms of OP. In particular, a number of biomarkers reflecting different aspects and levels of bone physiology and disease are now available.

DSA is a promising methodology which combines all the insights gained from these different but complementary approaches, via computational modelling. DSA aims to include the major signalling mechanisms and the experimentally observable results (e.g., temporal or spatio-temporal data on biomarkers) in order to create a mechanistic view of the underlying bone physiology and disease progression. Purely experimental approaches establish statistical correlations between individual risk factors and disease progression biomarkers. Mechanism-based models instead, allow for the integration of different factors into a comprehensive model of bone remodelling, providing a more holistic view of the disease progression and the effect of interventions. Moreover, once that the computational model has been developed, it can either be used to predict outcomes or as hypothesis generating tool to design new experiments [120].

Traditionally, PK/PD modelling was used to characterise the time course of a drug effect with the primary objective of optimising the dosing regimen and the delivery profile. Recently, PK/PD models have also been applied in the drug development process [41, 124]. The approach of conventional PK/PD models is descriptive, empirical and driven by a large amount of data. Due to their nature, these models are not able to predict clinical responses beyond the data which they are based on. For this reason, mechanism-based PK/PD models have been developed [41, 126, 147]. These are more sophisticated models which take into account the underlying mechanisms of a pathology and the action of the drug, with the aim of characterising the intermediate processes between the drug administration and the drug effect. This

characterisation relies on biomarker data and on two categories of parameters: the ones describing the properties of the drug (e.g., affinity and target activation) and the ones describing the properties of the biological system [40, 41, 124]. The separation between drug and system is crucial for the prediction and the extrapolation of treatment effects, in particular when the model takes into account disease-modifying agents that specifically target the underlying time course of the disease.

Nevertheless, both PK/PD and DSA models have had, so far, limited success in predicting fracture risk in osteoporotic subjects. Potential limitations of these approaches can be the non-detailed modelling of the underlying mechanical properties of bone, and the use of temporal assessment alone to study the effects of anti-catabolic and anabolic drugs on bone biomarkers. With the continuous improvement of bone imaging technologies, however, different spatial regions can be distinguished in bone and local BMD or bone volume (BV/TV) can be monitored. Given that bone structural properties strongly depend on the spatial distribution of BV/TV, understanding the effects of drugs on spatial changes is critical.

Here we will present our group effort over the past years to incorporate bone mechanical behaviour in mechanism based PK/PD models and extend the DSA approach to spatio-temporal models. In Sect. 2 we introduce the basic principles of bone physiology including: (i) a summary of the hierarchical structure of bone material; (ii) the mechanical and physiological function of bone modelling and remodelling; (iii) the major cell-cell signalling pathways; (iv) the mechanical and hormonal regulatory factors controlling bone homeostasis. In Sect. 3 we introduce the notion of bone biomarkers which provide the *signature* of a particular bone in terms of bone mass and turnover. The latter parameter indicates the amount of bone replaced in a certain period of time and can be used in the characterisation of bone homeostasis and bone diseases such as OP. Biomarkers will be discussed with respect to their catabolic or anabolic characteristics. BMD is discussed with respect to different measurement technologies. In Sect. 4 we discuss bone pathologies, in particular age-related bone loss and OP. Diagnosis and currently available treatment options are also described in this section. DSA in the context of conventional PK/PD models is reviewed in Sect. 5, introducing the notion of linear and asymptotic disease progression models together with symptomatic and protective disease interventions. In Sect. 6 we extend the concept of PK/PD modelling in bone with respect to mechanism-based PK/PD models and we introduce the bone remodelling model by Pivonka et al. [121] and extensions thereof. This mechanistic PK/PD model contains specific expressions of signalling pathways, hormones and growth factors that allow to quantitatively characterise processes and interactions from the drug administration to its effect. As an example, we show the effect that the anti-catabolic drug denosumab has on PMO. Finally, in Sect. 7 we provide a summary of the chapter with future directions in the application of DSA in OP research with emphasis on spatio-temporal modelling.

## 2 Relationship Between Structure and Function of Bone: An Overview

### 2.1 Bone Structure and Function

#### Material Characterisation: Organic/Inorganic

The skeletal system is a major constituent of the human body. It is an extensive connective tissue composed of bones, tendons, ligaments and cartilage. Bone is a dynamic living tissue which refers to a family of materials with different structural motifs, but all having in common the mineralised collagen fibril as the basic building block [170]. These materials have evolved to fulfil a variety of mechanical functions for which the structures are fine-tuned and adapted. Bone structure is highly complex and it can be described by up to seven hierarchical levels of organization (Fig. 1) [129]. The basic building block of bone, i.e., the mineralised collagen fibril, is composed of three major components. The first component is the *organic* part, mainly composed of Type I collagen present in the structural form that can also be found in skin, tendon and other soft tissues. Collagen constitutes the main component of the osteoid matrix (with proteoglycans and non-collagenous proteins forming additional constituents) into which, and in some cases onto which, the mineral forms. The second component is the bone mineral, which represents the *inorganic* part of bone tissue composed of dahllite, also known as carbonated apatite ( $Ca_5 (PO_4, CO_3)_3 (OH)$ ). Water represents the third component. During the biological process of bone remodelling (see also Sect. 2.2), osteoblasts and osteocytes assemble these three components into an ordered structure known as mineralised collagen fibril.

#### Cortical and Trabecular Bone

Based on morphological structure, mechanical properties and metabolic functions, two types of bone can be distinguished: *cortical* and *trabecular* (Fig. 1). Cortical or dense bone forms the outer shell of bones. It consists of layers of bone (i.e., lamellae) organized around a central canal in which blood vessels, nerves, connective tissue and lymphatic vessels are found. This functional unit is referred to as Haversian system or osteon. Approximately 80% of the skeletal mass is cortical bone. On the other hand, trabecular or cancellous bone consists of an interconnected network of struts and plates. Pore spaces within this network are filled with blood vessels, nerves and bone marrow. Trabecular bone is found at the distal end of long bones, in short bones, in the inner surfaces of flat bones and in irregular bones such as vertebrae. Approximately 20% of the skeletal mass is trabecular bone.

#### Bone Mechanical Properties, Bone Quality and Fracture Risk

Cortical bone is a dense calcified tissue having high resistance to bending and torsion. It provides mechanical strength and protection to vital internal organs and bone marrow. Cortical bone also forms the basis for muscles attachment, supporting locomotion. On the other hand, trabecular bone is less dense and composed of thin

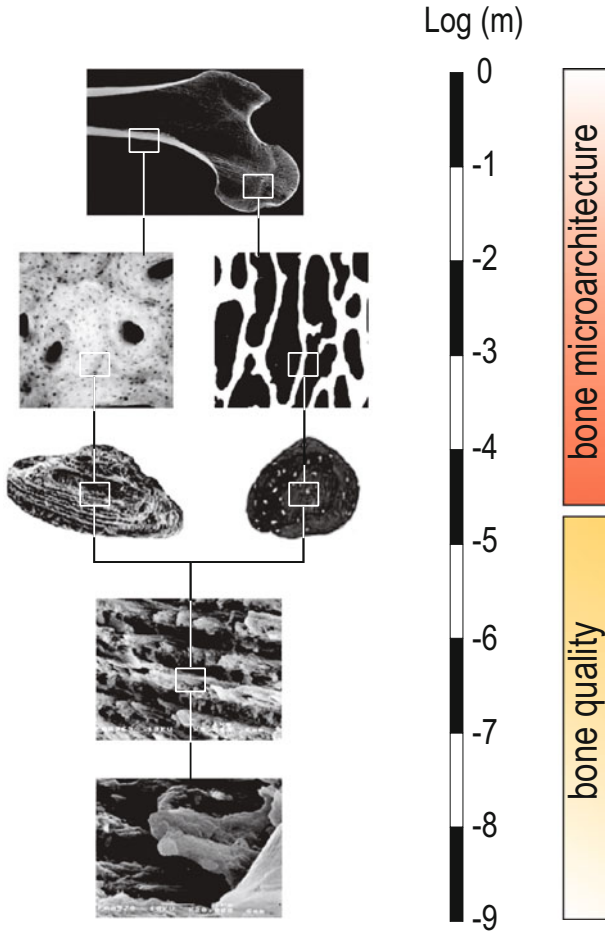


**Fig. 1** Hierarchical structure of bone: from whole organ scale (cortical and cancellous bone) to cylindrical arrangements in osteons and features of bone quality (composition and arrangement of mineralised collagen fibrils, size of bone mineral crystals, collagen molecules and non-collagenous proteins)

trabeculae which form a robust 3D structural framework with elastic properties. It contributes to provide mechanical support, particularly in bones such as vertebrae, femoral head and neck. Due to its high turnover rate, trabecular bone has a major function in metabolic processes serving as a reservoir of calcium and phosphate for the maintenance of mineral homeostasis (see also Sect. 2.2). Cortical bone instead, is involved in metabolic processes only in situations of severe or prolonged mineral deficit [58, 87, 150].

In order to determine the biomechanical function of bone, mechanical testing is commonly applied. Traditional mechanical testing provides detailed information on

the whole-bone mechanical properties and on the properties of the matrix material, however, it does not reveal local failure characteristics. High correlation has been established between the elastic properties of bone and its density [27]. Utilising multiscale modelling techniques based on micromechanics, it is now possible to link individual bone constituents in a hierarchical way so that anisotropic elastic properties of bone can be predicted [60]. A correlation has also been shown between bone strength and bone density [27]. However, computational prediction of bone strength is challenging because of the non-linear and inelastic material behaviour of bone tissue. Bone failure is a complex process that depends on: (i) the applied loading regimen (uniaxial vs. multiaxial); (ii) the loading rate (static vs. dynamic); (iii) the structural and material properties. When exposed to a slow and monotonous loading condition, bone initially deforms elastically. After reaching the yield limit, the deformation becomes inelastic. Close to the ultimate load (i.e., maximum structural load) high local deformations occur, together with local growth and propagation of microcracks that eventually lead to a macroscopic failure [103]. Another important quantity characterising bone resistance to failure is the bone toughness, i.e., the integral of the stress-strain curve in the post elastic regimen [134]. During ageing, bone becomes more brittle due to the loss of ultrastructural water in the bone matrix that significantly reduces bone toughness [113]. Furthermore, anti-resorptive drug treatments have been associated with increased brittleness of bones [153]. Although some work has been done to clarify the characteristics of bone failure, fundamental knowledge on how failure originates within trabecular and cortical bone is still lacking. However, to be able to estimate the fracture risk of a specific patient, a detailed understanding of bone failure behaviour is essential.

The emergence of accurate and precise bone densitometry over the last two decades resulted in bone density becoming a primary target in the diagnosis and monitoring of OP. Bone strength and fracture risk are generally assessed by measuring BMD. Although large population studies demonstrated a strong correlation between bone density and bone mechanical properties of trabecular bone [149, 164], bone mechanical properties also depend on the architecture and the intrinsic material properties of the tissue [25]. In fact, the risk of fracture in a 75 year old woman is 4–7 times higher than the risk of fracture in a 45 year old woman having the same bone mass [68]. This demonstrates that bone fragility is not determined by bone mass only. In agreement with this idea, it has recently been observed that all the anti-resorptive treatments for OP have about the same fracture efficacy, although there is a seven-fold difference in their effect on BMD. Consequently, it is difficult to achieve an accurate assessment of bone fracture risk in a clinical environment solely on the basis of bone densitometry. Other factors such as bone microarchitecture, bone turnover (i.e., proportion of bone replaced in a certain unit time, usually expressed as %/year), microcrack and microdamage distributions and bone matrix material properties also have important roles. All these factors, together with BMD, are often referred to as *bone quality* [25]. In the following, two factors of bone quality, i.e., bone turnover and degree of mineralisation of bone tissue, will be discussed in the context of bone physiology and pathology.

## 2.2 Bone Physiology

Bone has multiple functions within the body. Among these, the most important one is to enable locomotion by providing support to muscles, ligaments, tendons and joints. To carry out this function, bone needs to maintain structure and strength with minimal weight. Bone also provides a readily accessible store of calcium to support calcium homeostasis. Other roles of bone include: providing a protected environment for bone marrow, providing support for a haematopoietic stem cell niche [26], acting as an endocrine organ regulating energy metabolism potentially via osteocalcin [31].

### Bone Modelling and Remodelling

To accomplish all its functions, bone needs several cellular mechanisms. To meet the biomechanical demand, for example, bone requires a control system able to detect bone strain and/or other mechanical quantities (e.g., hydrostatic pressure and fluid flow) and microdamage. Signalling systems inducing a reparative response, i.e., inducing bone resorption to remove damaged bone and bone formation to replace it with new one, are also needed [80]. The main processes by which bone is able to continuously adapt and renew in response to biomechanical and metabolic demands are *bone modelling* and *bone remodelling*.<sup>1</sup>

Bone modelling refers to the process in which bone formation and bone resorption occur at spatially distinct sites [7, 72]. It shapes skeletal elements and ensures the acquisition of the appropriate bone morphology and mass during growth. Bone modelling occurs at a low rate throughout life. It is required for both bone repair and bone adaptation to mechanical loading, being the latter in control of the size, structure and shape of bones.

On the other hand, bone remodelling refers to the process of bone renewal in which bone resorption and bone formation occur spatially at the same site and turn bone tissue over at regular intervals. In remodelling, bone resorption and formation are coupled, occurring in packages of cells along specific sites on the same bone surface. This warrants that old bone sites that have been resorbed will be filled with new bone. While bone modelling predominantly occurs in the growing skeleton, bone remodelling occurs throughout life. Moreover, bone remodelling has been suggested to regulate calcium and phosphorus homeostasis and to repair microcracks.

### Bone Cells in (Re)modelling

To translate local mechanical and autocrine/paracrine biochemical signals into tailored bone remodelling responses, certain requirements need to be fulfilled. Less structurally important bone, for example, should be targeted for calcium mobilization during times of high calcium demand [93]. To achieve all the diverse requirements, three bone cell types are present in bone microenvironment:

---

<sup>1</sup>Following the notation of L. Lanyon we will use (re)modelling to denote both modelling and remodelling.

*Osteocytes* reside within the bone matrix. They interact with the surrounding bone matrix and communicate to adjacent osteocytes via a dense and interconnecting canaliculi network which contains osteocyte cell processes. Osteocytes orchestrate the detection and the response to microdamage, fracture, and changing bone strain. They represent about 90% of all bone cells [84].

*Osteoblasts* are cells of mesenchymal origin which line the surface of bone. They form bone by progressive bone matrix deposition and subsequent mineralisation. Cells of this lineage have receptors for parathyroid hormone (PTH), 1,25-dihydroxyvitamin D, and a number of local regulatory factors [136]. After completing the bone formation process, these cells can either undergo apoptosis (i.e., cell death), remain on the newly formed bone surface and become lining cells, or be trapped in the bone matrix and further differentiate into osteocytes.

*Osteoclasts* are large multinucleated cells of haematopoietic origin able to resorb bone. Adhering to bone surface, they secrete acid to demineralise bone and proteolytic enzymes to break down the collagenous bone matrix [22, 165]. Osteoclasts are typically unable to respond directly to pro-resorptive hormones and require the presence of osteoblasts to locally regulate their differentiation and activity.

Communication between osteocytes, osteoblasts and osteoclasts enables a spatio-temporal coordinated response to both physiological and pathological demands via the integration of multiple catabolic and anabolic signals. Bone cells are organised into clusters named *basic multicellular units* (BMUs) by Frost who was the first to describe them as the basic functional unit of bone remodelling [44, 50, 51]. In a normal adult skeleton, there are about  $1.7 \cdot 10^6$  BMUs [50, 52, 169]. At the front of a BMU, osteoclasts dissolve the bone matrix creating a resorption cavity (also known as cutting cone). Towards the rear of a BMU, osteoblasts secrete osteoid, an organic matrix of collagen fibres gradually refilling the resorbed cavity. This organic matrix becomes gradually mineralised and forms new bone (Fig. 2). The osteoid mineralisation process is believed to be partly regulated by osteoblasts and osteocytes. In cortical bone, BMUs proceed through the bulk of the tissue leaving new secondary osteons in their wake. Osteons are cylindrical tissue structures having a diameter of about 100–200  $\mu\text{m}$ , have a length of up to 10 mm and are aligned with the main loading direction [85, 159, 160]. In trabecular bone, BMUs proceed along the surface of plates and struts, forming hemi-osteons or trenches of new bone tissue about 60–70  $\mu\text{m}$  deep [159].

Since trabecular bone remodelling operates on bone surface, it can be associated with either negative bone balance (net bone loss) or positive bone balance (net bone gain). In cortical bone the situation depends on the mode of remodelling: if a new Haversian canal (type I osteon) is created, the remodelling process always implies net bone loss; if a pre-existing Haversian canal (type II osteon) is used, net bone gain occurs if the diameter of the Haversian canal is reduced by the passage of the BMU [116, 135]. The exact proportion of type I over type II osteons in cortical bone remodelling is controversial, in fact, vascular channels increase with age [116], but age-related bone loss is due to increased pore area rather than increased pore density [167].

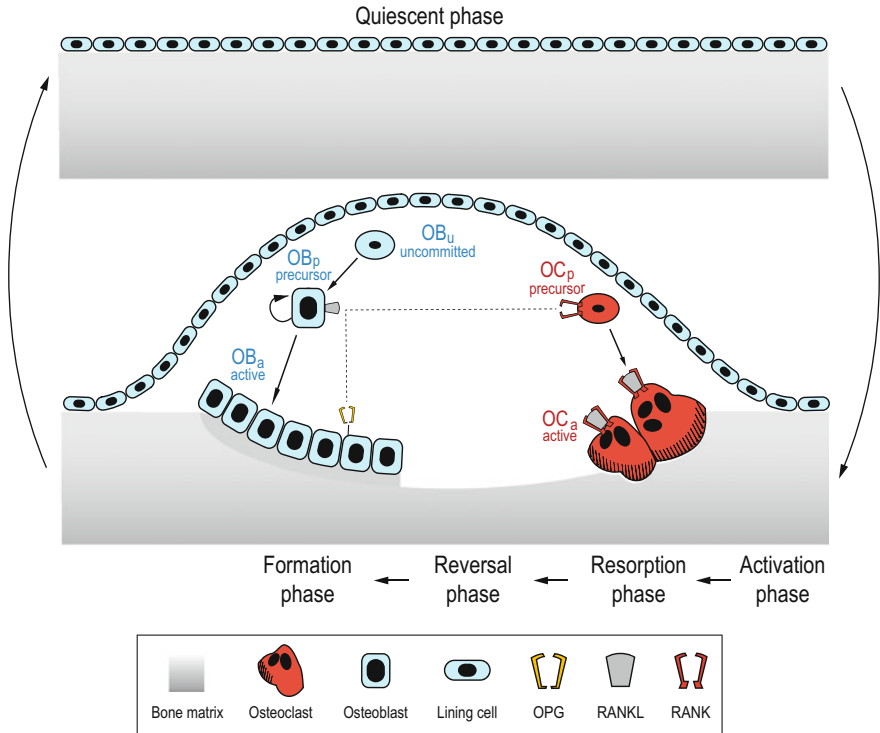


**Fig. 2** Bone remodelling and BMU on a trabecular bone surface: bone lining cells retract from bone surfaces and form a closed canopy over the remodelling site (activation phase), osteoclasts remove bone (resorption phase), bone surface is prepared for bone formation (reversal phase), osteoblasts form bone matrix (formation phase) and eventually either undergo apoptosis, become enclosed in bone to develop into osteocytes or differentiate into lining cells (return into a quiescent phase)

Dynamic histomorphometry techniques, such as tetracycline labelling and radionuclide imaging, have considerably helped in the elucidation of kinetic properties of matrix apposition and cell development within BMUs [69, 70, 118]. Whilst trabecular bone exhibits the same sequence of surface activation, resorption and formation, its three-dimensional organisation is difficult to visualise from two-dimensional histological sections. Latest imaging techniques apply synchrotron radiation (SR micro-CT) to visualize the morphology of 3D osteonal structures ex vivo [33]. Phase-contrast agents have been used in combination with SR micro-CT to visualize osteonal structures in vivo [59].

### Cell Signalling Pathways and Regulatory Factors (Mechanical, Hormonal, Local)

#### *Catabolic pathway: RANK-RANKL-OPG*

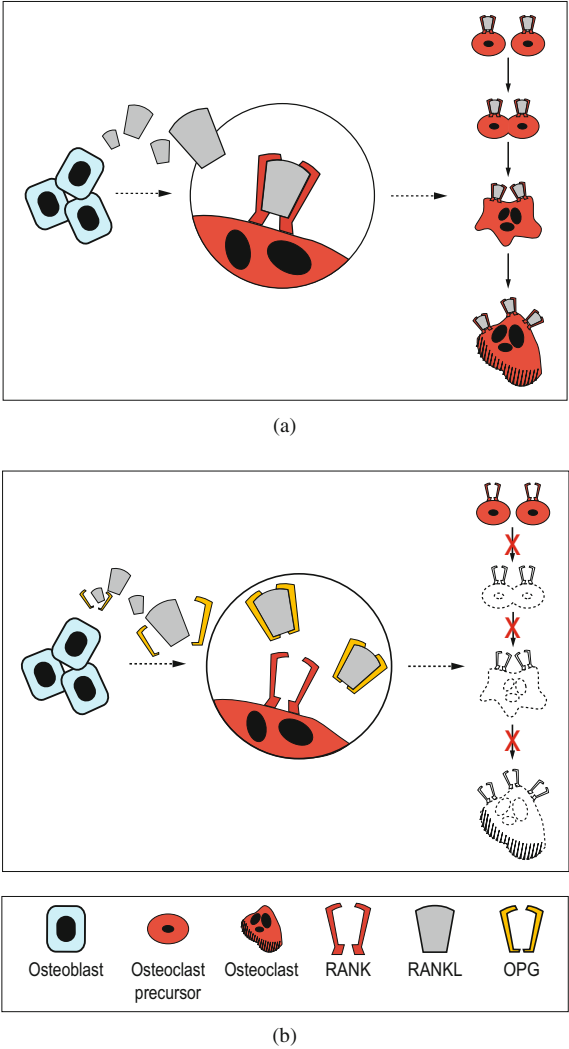
Bone resorption is regulated via the integration of multiple pro- and anti-resorptive stimuli with convergence of output into a dominant mediating pathway. Cells of

the osteoblast lineage integrate hormonal, mechanical and pathological signals that change their expression of the cytokine receptor activator of nuclear factor kappa-B ligand (RANKL) [82, 176] and its inhibitor osteoprotegerin (OPG) [157, 168]. RANKL is either expressed as a membrane bound cytokine or released in a soluble form by cells of the osteoblast lineage. Osteocytes, osteoblasts and osteoblast precursors can express RANKL and currently there is some controversy regarding which predominate. Apparently, selective knock-down of RANKL in osteocytes produces a moderately severe osteopetrosis in mice, indicating that osteocytes have a significant role as source for RANKL [108]. RANKL binds to its receptor RANK (receptor activator of nuclear factor kappa-B) expressed on the surface of osteoclast precursor cells. The RANKL-RANK binding induces intracellular signalling pathways driving the differentiation into an osteoclast phenotype, activating osteoclastic bone resorption and increasing osteoclast survival (Fig. 3a) [107]. OPG is a decoy receptor for RANKL naturally secreted by cells of the osteoblast lineage and involved in the regulation of the resorption process. OPG, in fact, binds to RANKL to prevent its association with RANK. Consequently, osteoclast differentiation and activity are inhibited and osteoclast apoptosis is promoted (Fig. 3b). Therefore, if RANKL expression exceeds OPG expression, bone resorption is promoted, vice versa, if OPG expression exceeds RANKL expression, bone resorption is inhibited (<http://www.rankligand.com/>).

Pro-resorptive hormones, such as PTH and calcitriol, increase RANKL expression within bone and decrease the OPG one, leading to increased bone resorption. These hormones and other local regulatory factors bind to their own specific receptors expressed on osteoblasts and activate signalling pathways leading to an increased RANKL expression. On the other hand, bone protective agents such as estradiol and testosterone tend to increase the expression of OPG relative to RANKL, reducing bone resorption [67, 101]. Local regulatory factors such as PTHrP, IL-1 and TNF- $\alpha$  increase the expression of RANKL on cells of the osteoblast lineage in case of pathological bone loss related to cancer (PTHrP) or inflammation (IL-1 and TNF- $\alpha$ ). Local regulatory factors such as mechanical signals, on the other hand, alter RANKL and OPG expressions in a spatially restricted manner. Reduced bone strain and the presence of either microfractures or fatigue damage increase the RANKL/OPG ratio, while increased bone strain tends to decrease the RANKL/OPG ratio via osteocytes [81].

While RANKL-RANK signalling is necessary and dominant in the regulation of bone resorption, other modulating molecules can directly signal osteoclasts to magnify or diminish their response to RANKL. Inflammatory cytokines, for example, can enhance the osteoclast response [83]. In contrast, the systemic hormone calcitonin inhibits (reversibly) the osteoclast response via the activation of the calcitonin receptor on mature osteoclasts [28]. In addition, there are other sources of RANKL in bone that tend to contribute to the regulation of bone resorption during disease. Activated T-cells, in particular, secrete RANKL and can induce bone resorption during infection or chronic inflammation [166].

**Fig. 3** Role of the RANK-RANKL-OPG pathway in osteoclastogenesis: osteoblasts express RANKL on either cell surface or in soluble form (shown here). **a** Osteoclastogenesis is promoted by osteoblasts via the RANKL-RANK binding which induce osteoclast precursor cells to differentiate into active osteoclasts. **b** Osteoclastogenesis is inhibited by osteoblasts via the production of OPG which blocks RANKL-RANK interactions [22]



*Anabolic Pathway: Wnt Signalling*

The Wnt family of growth factors, together with their receptors, co-factors and inhibitors, represent one source of regulation of both the mesenchymal stem cell lineage commitment and the osteoblast precursors population. There is evidence that mature osteoblasts can secrete Wnt that in turn acts on early mesenchymal precursors to induce differentiation in the osteoblast lineage [7]. However, the understanding of the Wnt action is complicated due to the presence of 19 Wnt ligands, 10 Wnt receptors and multiple Wnt receptor co-factors and inhibitors [77]. Another contribution to lineage commitment for osteoblast precursors may come from bone morphogenetic proteins (BMPs), a group of growth factors produced by osteoblast lineage cells and

sequestered in bone matrix [1]. However, it is difficult to separate this action from their differentiation activity. During the inflammation typical of fracture repair, the transient exposure to  $\text{TNF-}\alpha$  may also influence the commitment of mesenchymal stem cells to the osteoblast lineage [95].

### Association Between Bone Remodelling and Bone Mineralisation

The measurement of the degree of mineralisation of bone (DMB), also known as tissue mineral density (TMD), is relatively recent compared with the assessment of bone vascular porosity. The most accurate way to assess TMD is microscopically (i.e., at the bone matrix level) using high-resolution imaging techniques. This approach translates the linear X-ray attenuation coefficient for a given beam energy in grey level values in the 3D reconstructed micro-CT or SR micro-CT images [112, 139]. The X-ray attenuation depends on the material composition and in a bone sample it is related to the mineral component of the bone. The amount of mineral per unit volume of bone matrix (in  $\text{g/cm}^3$ ) in a bone sample can be estimated using a calibration technique based on *phantoms* of known compositions. These calibration phantoms can either be solid and made of different concentrations of calcium hydroxyapatite ( $\text{CaHA}$ ) or liquid and made of homogeneous solutions of water and different concentrations of dipotassium hydrogen phosphate ( $\text{K}_2\text{HPO}_4$ ) [109]. The distribution of the grey levels within different regions of interest (ROIs) can be obtained from the histogram of the bone images normalized by the total volume (TV).

TMD has been directly associated with bone mechanical properties either at the bone structural unit level [150, 161] or at the whole bone tissue level [38, 39, 47]. Moreover, TMD has also been associated with the bone remodelling activity (Fig. 4a) [4]. According to the model recently developed by Bala and co-workers, an increase in bone remodelling leads to an increase of BMUs birthrate and to a decrease in TMD related to the lower probability to complete the secondary mineralisation, being the latter a slow phase of mineralisation which can take up to several years with a large fraction completed within one year [3, 18, 140, 141]. In case of hyperparathyroidism, for example, the proportion of bone structural units (BSUs) undergoing primary mineralisation decreases, the mean TMD decreases and its distribution broadens (Fig. 4b). The opposite occurs when the remodelling activity is low or reduced due to drugs and/or pathologies (Fig. 4b). In this case, the different BSUs have more time to complete mineralisation before being resorbed in a further remodelling event [16]. As a consequence, the proportion of bone highly mineralised maximally increases and its distribution becomes more homogeneous, the mean TMD increases and its distribution narrows [19, 137]. This conceptual model has been widely validated by the observation of pathologies and drugs altering remodelling activity.

In normal bone, the evolution of TMD with age has been widely studied and the overall result is the absence of correlation with age. More generally, it has been found that the TMD mean was age, sex, race, bone site and bone envelope independent and that the inter-individual variation was low [8, 11, 17, 48, 138]. However, some studies revealed a positive correlation between TMD and age [49, 138, 163]. This discrepancy may have several causes. Among these, one example is the fact that most of the samples were collected at the autopsy or drawn from anthropologic

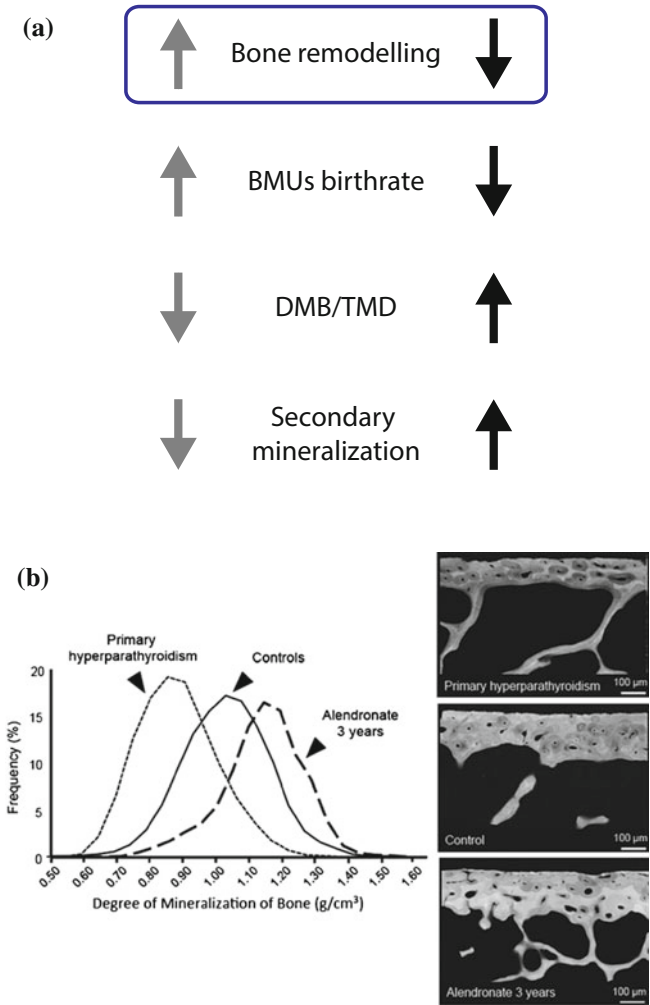


**Fig. 4** Bone mineralisation and bone turnover: **a** the degree of TMD is regulated by the rate of bone turnover, higher turnover rates lead to lower TMD and vice versa. **b** Bone diseases characterised by high bone turnover rates (e.g., primary hyperparathyroidism) lead to a decreased TMD, anti-catabolic drugs (e.g., Alendronate) inhibit bone turnover and result in increased TMD, modified from [4] with permission

collections with few medical history details. Moreover, anthropologic collections comprised specimens from populations in the ninetieth century (before the industrial revolution) which are not representative of our modern population [11]. Another cause of the discrepancy can be that age classes are often not well balanced, with fewer individuals in both youngest and oldest categories. Furthermore, most of the results are reported on iliac crest samples because they are easier to collect. However, even if data suggest that changes in the iliac crest are correlated to the changes in

other bone sites with a mixture of cortical and trabecular bone, e.g., femoral neck and vertebral bodies [42, 127], extrapolations to the femoral shaft are limited. In fact, the differences between femur and iliac crest are striking: the femur is a weight bearing bone, entirely cortical and a site of osteoporotic fracture, all characteristics that are absent in the iliac crest. Another cause of discrepancy can be the fact that most of the studies investigated the cortical bone as a homogeneous bulk, masking the radial and circumferential regional inhomogeneities. A recent study highlighted that the DMB assessed in the femoral midshaft using SR micro-CT decreased from the periosteal to the endosteal surface [144]. Further investigations regarding spatial inhomogeneities of TMD are required.

### 3 Biomarkers Characterising Mass, Quality and Turnover of Bone

Currently, there is no standard practice to monitor patients receiving treatment for OP. Repeated dual-energy X-ray absorptiometry (DXA) is a diagnostic test commonly used to assess the change in BMD following a therapeutic intervention. However, this technology has several limitations such as long time interval between two consecutive BMD measurements (6–9 months are needed to be able to detect changes in BMD), limited access to the DXA machine, elevated cost of the technology and low correlation between BMD monitoring and fracture risk estimate. A recent review pointed out that BTMs measuring bone resorption and formation may offer an alternative monitoring strategy [61]. Some advantages that BTMs have over DXA in monitoring the response to OP therapies are, for example, their non-invasive nature, their relatively cheap cost and the capability to detect changes in bone turnover rates after 3–6 months of therapy and in some cases already after 2 weeks.

More generally, these clinical quantities used to characterise OP and therapeutic interventions can be divided in two groups: *specific biomarkers* and *non-specific biomarkers*. Specific biomarkers such as BMD are specific to a particular bone site (e.g., femoral neck, lumbar vertebra, wrist) and reflect the effects of disease and treatment as changes in BMD over time. On the other hand, BTMs are non-specific biomarkers as they reflect bone remodelling activities in the whole skeleton and, as such, they are not specific to a particular bone site. In the following, we will review the use of these biomarkers in the context of OP and various therapeutic interventions having in mind to use these quantities for DSA.

#### 3.1 Bone Structure and Bone Mineral Density

Imaging is essential to the evaluation of bone and joint diseases. In this context, many studies were conducted in order to find non-invasive analytical techniques to quantify

the changes occurring in bones and joints over time, both in health and disease [103]. Several methods are used to measure BMD at different skeletal sites, such as ultrasound, radiographic absorptiometry, dual photon absorptiometry, quantitative computed tomography (QCT), quantitative ultrasound and DXA [37, 76, 174]. The application of a particular technique depends on the accessibility of a particular bone site. In particular, latest high resolution QCT (HR-pQCT) techniques can mainly be applied at sites of the peripheral skeleton such as wrist and proximal tibia.

The gold standard in clinical practice for the assessment of BMD is DXA, which measures the mineral content of bone per unit area (in  $\text{g}/\text{cm}^2$ ) involving a low radiation exposure. The most relevant sites for the clinical assessment of the fracture risk using DXA are the spine (predominantly trabecular), the hip (mixed trabecular-cortical) and the wrist (predominantly cortical), and are routinely assessed using this technology to monitor the changes in BMD [173, 174]. One major drawback of DXA is that cortical and trabecular bone cannot be distinguished. DXA calculates BMD using a projected areal density (i.e., 2D image) and it does not measure a true density [158]. Hence, the quantification of bone structure, material composition or cortical porosity is not possible with this technology.

HR-pQCT is an imaging technique that allows to better understand bone and joint diseases at the microarchitectural level. It provides high resolution 3D images ( $82\text{ }\mu\text{m}$  isotropic voxel size) using a relatively low radiation dose ( $3\text{--}5\text{ }\mu\text{Sv}$ ) compared to total body CT scans [56]. With this technology, properties and microarchitecture of cortical and trabecular bone can be analysed separately. It also allows the in vivo assessment of the spatial distribution and dimension of cortical bone erosions. Furthermore, micro-finite element analysis (micro-FEA) can be performed on HR-pQCT data to calculate bone mechanical properties at the distal sites of the skeleton (i.e., distal radius and distal tibia). HR-pQCT can also be used to evaluate patient specific drug effects on bone.

BMD and structural parameters of bone such as trabecular thickness (Tb.Th) and trabecular numbers (Tb.N) are specific biomarkers that can be used to assess the changes in bone microarchitecture due to OP. One example of specific bone biomarkers is shown in Fig. 5a where micro-CT reconstructions of biopsy specimens of the iliac crest at baseline (left) and after three years (right) clearly show that both cortical and trabecular bone become thinner and connectivity is lost with the disease progression in an untreated patient [150].

### 3.2 Bone Turnover Markers

BTMs characterise the dynamic activity of bone cells via measurements of their biochemical concentrations in blood, serum or urine. BTMs are defined as non-specific biomarkers of bone because they provide information related to the whole body as opposed to site-specific information on a particular bone site. For this reason, the effectiveness of a particular treatment needs to be evaluated carefully. BTMs can be distinguished in three different types according to their relation to bone (re)modelling

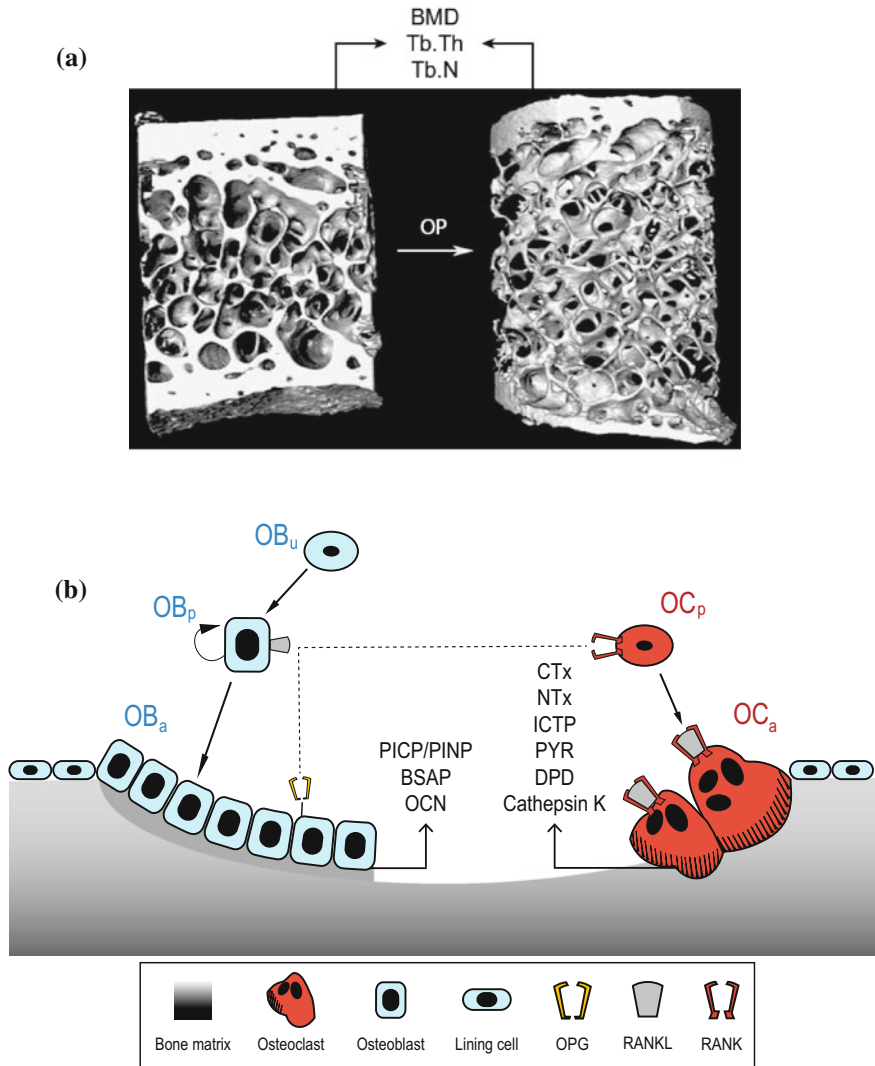


**Fig. 5** Biomarkers reflecting bone physiology: **a** specific biomarkers such as BMD, Tb.Th and Tb.N, from micro-CT images of biopsy specimens of the iliac crest at baseline (*left*) and after 3 years (*right*), modified from [150]. **b** Non-specific biomarkers of bone turnover in relation to their origination during bone remodelling process

activity: (i) collagenous bone resorption markers, (ii) bone formation markers, (iii) markers of osteoclast regulatory proteins [36, 87, 151]. An overview of various markers of bone turnover in relation to their origin and function is provided in Fig. 5b and Table 1 [125]. Collagenous resorption markers are degradation products of bone collagen and their concentrations reflect the rate of bone resorption [36, 151]. Bone formation can be measured based on the enzyme activity of osteoblasts, on the bone protein composing the bone matrix and on the pro-collagen markers. Osteoclast regulatory proteins are divided into markers reflecting the rate of osteoclastogenesis and the osteoclast numbers. Measurements of calcium and phosphate concentrations provides additional information on bone turnover and reflect the net balance between bone resorption and bone formation in the whole body [104]. It is worth to mention that calcium balance studies are costly, time consuming and difficult to perform [117].

BTMs have advantages over BMD measurements as they are non-invasive, relatively cheap and can detect changes in bone turnover rates earlier. However, the disadvantage of a particularly high within- and between-patient variability needs to be taken into account when using BTMs. Moreover, their ability to identify treatment non-responders and predict future fracture risk has yet to be established.

### ***3.3 Characteristic Time Scale and Variability of Bone Biomarkers***

In order to use bone biomarkers in the diagnosis and treatment of OP and other bone disorders, it is important to understand the dynamics and the variability of BMD and BTMs due to both technical and biological causes. From the technical point of view, variability in BMD measurements depends on the type of device used (e.g., lunar or hologic DXA scanners). The precision of a measurement can vary due to device errors, technician variability, intra- and inter-observer variability and between-centre variations [15, 43]. Nevertheless, the overall reproducibility of DXA measurements has been proven satisfactory with phantom measurements [155]. To overcome the issues of comparing numerical measures of BMD obtained from different scanners, each device manufacturer provides the user with a reference distribution that allows to internally normalize the individual measure with respect to the peak bone density of young adults. This normalised parameter is known as T-score and represents the number of standard deviation (SD) of the BMD measurement above or below the BMD of a young healthy adult of the same sex. The use of the T-score allows a better comparison between measurements taken with different scanners. To evaluate the precision error, repeated scans are performed on a set of patients and the reproducibility is characterised. Generally, this characterisation take place over a short period of time (about 2 weeks) so that no real change in the BMD is expected and the short-term precision error is quantified [43]. The BMD precision error can be expressed as coefficient of variation (CV [%]), which is the ratio of the SD to the

**Table 1** Non-specific biomarkers of bone turnover [125]

Marker	Sample	Remarks
<b>Bone resorption</b>		
<i>Collagenous bone resorption markers</i>		
CTx	Urine and serum	Bone degradation products reflecting resorption and composition rates.
NTx	Urine and serum	Bone degradation products reflecting resorption and composition rates.
ICTP	Serum	Bone degradation products reflecting resorption and composition rates.
PYR/DPD	Urine and serum	Bone degradation products reflecting resorption and composition rates, derived from mature type I collagen.
<b>Bone formation</b>		
<i>Enzyme activity marker</i>		
BSAP	Serum	Osteoblast products, related to osteoblast and osteoblast precursor activity, involved in bone mineralisation.
<i>Bone protein marker</i>		
OCN	Serum or plasma	Non-collagenous protein of bone matrix, osteoblast products, bone degradation product, correlated to histomorphometric measurements.
<i>Pro-collagen marker</i>		
PICP/PINP	Serum or plasma	Osteoblast and fibroblast proliferation, released from newly synthesized pro-collagen, PINP correlates to histomorphometric measurements.
<b>Osteoclast regulatory proteins</b>		
<i>Markers of osteoclastogenesis</i>		
RANKL	Serum	Active osteoblasts and activated T-cells products.
OPG	Serum	Osteoblasts products.
<i>Markers of osteoclast numbers</i>		
Cathepsin K	Serum or plasma	Type I collagen degradation enzyme.
CTx = C-terminal cross-linked telopeptide of type I collagen; NTx = N-terminal cross-linked telopeptide of type I collagen; ICTP = C-telopeptide pyridinoline cross-links of type I collagen; PYR = pyridinoline; DPD = deoxypyridinoline; BSAP = bone-specific alkaline phosphatase; OCN = osteocalcin; PICP = C-terminal pro-peptide of type I collagen; PINP = procollagen type I N-propeptide; RANKL = receptor activator of NF- $\kappa$ B ligand; OPG = osteoprotegerin.		

mean of the measurement, or as SD  $[\text{g}/\text{cm}^2]$ . Studies have shown that the short-term precision error in SD for lumbar spine and total hip is constant and ranges from 0.01 to  $0.15 \text{ g}/\text{cm}^2$ , corresponding to a CV between 1 and 1.5% with  $1 \text{ g}/\text{cm}^2$  used as reference [175]. This implies that CV increases with decreasing BMD. Therefore, when assessing for significant changes in BMD, it is common practice to use SD rather than CV. The reproducibility of a measurement can also be quantified measuring the smallest detectable difference (SDD) that represents the minimum meaningful BMD change that can be detected with a certain device. The SDD is measured using the Bland and Altman's 95% limit of agreement method [14, 43] and is generally preferred to CV because is expressed in absolute units  $[\text{g}/\text{cm}^2]$  and is independent of the BMD level. It has been shown that in older subjects, the measurement error increases for the spine and total hip. The long-term precision error in a clinical study increased by 6.5–9.2% with each additional year of monitoring [142].

Biological variability reflected in BMD measurements instead, arise from the effect that factors such as age, sex, demographics, seasonal variation, recent fractures, drug treatment, disease, mobility and lifestyle (including diet and vitamin D intake) have on the underlying bone physiology [87, 151].

BTMs exhibit high intra- and inter-individual variability. The technical causes for this are determined by the type of marker measured, e.g., resorption markers are often a mixture of molecular entities, and the type and precision of the assay used to detect a specific marker. The CV for the inter- and intra-assay variability are typically within 10% [87]. Other technical sources of variability are the inter-laboratory variation, the mode of sampling (e.g., 24-h or second morning void for urinary markers), the timing of sampling (e.g., diurnal variation), the type of sample taken (e.g. urine or serum) and the status of the subject before the sample collection (e.g. fasting, exercised). To control all these factors it is necessary to have an appropriate study design, a specimen collection protocol and to use standardised assays and working protocols [151, 152].

On the other hand, the biological causes of variability in the measures of BTMs are more difficult to control. These are the same factors mentioned previously for BMD measurements, such as age, sex, recent fractures, drugs, disease, lifestyle and also temporal variability (e.g., diurnal variation, menstrual rhythm) [36, 151]. However, in contrast to BMD, the influence of several of these factors on BTMs concentration can be observed on a daily to monthly basis. In general, the variability in BTMs increases with age and after menopause.

In Sect. 6 we will discuss how a mechanistic model can aid in comparing disease and treatment effects based on these heterogeneous sets of biomarkers. This type of model captures the underlying dynamics present in the data independently of the measured markers, assays used and reported assay units. It can also detect differences in the methodology used to analyse the markers in different studies. In addition, the previously mentioned difference in BMD values due to different devices can be incorporated in a mechanistic model.

## 4 Bone Pathology: Osteoporosis and Treatments

OP and its related skeletal complications are amongst the most important diseases impacting on both quality of life of the ageing population and costs of the health care system. Bone diseases in the elderly, are associated with high morbidity and increased mortality. OP in particular, is characterised by low bone mass due to increased (macroscopic) porosity, which leads to the deterioration of bone microstructure. Cortical bone deterioration is characterised by an increased intra-cortical porosity and trabecularisation of endocortical bone regions. On the other hand, trabecular bone loses connectivity between trabecular struts and plates. Furthermore, OP changes the mechanical properties of the bone matrix. The increased mineralisation, in fact, induces a more brittle material behaviour. These changes in bone structure and quality enhance bone fragility and consequently the fracture risk [173].

Different types of OP can be distinguished: PMO, senile or age-related OP, idiopathic and juvenile OP, OP resulting from other diseases (e.g., hypogonadism, endocrine states, diabetes) or conditions in the mechanical environment (e.g., immobilization) and OP due to deficiencies (e.g., vitamin D, calcium) and medications (e.g., corticosteroids) [130, 132]. Among all these types, age-related OP and PMO are the most frequent ones. It is now well established that normal ageing leads to trabecular and cortical bone loss, in both women and men. This bone loss starts from the fourth or fifth decade of life onwards, with a more pronounced effect in women after menopause (Fig. 6). Due to this accelerated bone loss, prevalence of OP and probability of fractures beyond age 50 is about 3 times higher in women than in men [76]. In women, age-related bone loss starts approximately 10–15 years preceding menopause affecting primarily trabecular bone. A study measuring BMD using DXA suggested that cortical bone is not damaged until menopause [2], however, this might be related to limitations in the imaging resolution. Intra-cortical bone loss and how this is affected by oestrogen can be better investigated using latest technologies such as HR-pQCT [24, 56].

### 4.1 *RANK-RANKL-OPG Pathway*

As pointed out in Sect. 2.2, the RANK-RANKL-OPG pathway is responsible for catabolic regulations and if altered towards an increase in the RANKL/OPG ratio it leads to enhanced osteoclastic activity. This process has been associated with various metabolic bone diseases, including OP [64, 155, 172]. Age-related bone loss is thought to be a combination of several factors, which includes: reduced bone formation, cumulative effects of calcium and vitamin D deficiency, decreased physical activity, lack of mechanoresponsiveness of osteocytes and age-related decrease in gonadal function [143]. Deficiency in calcium and vitamin D has been associated with increased osteoclastic activity via the action of PTH [117]. To react to low levels of calcium in blood the parathyroid gland secretes PTH in excess (secondary

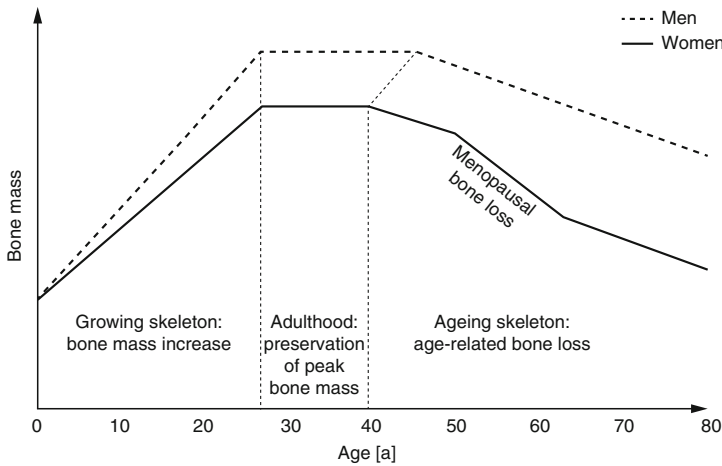


**Fig. 6** Bone mass variation with age in men and women: during growth bone mass increases reaching a peak at around 30 years of age (greater in men than in women). At around 40–45 years of age, age-related bone loss is observed in both men and women, but it is more pronounced in women (for about 10 years) due to menopause

hyperparathyroidism) to induce a calcium release from bone via osteoclastic bone resorption. This process is reflected in the variation of BTMs such as OPG and RANKL. On the other hand, it has been shown that serum OPG concentrations increase with age, both in men and women [78]. Although unexpected, this OPG increase does not exclude the possibility of bone site-specific increases in RANKL concentrations which drive bone resorption.

Oestrogen concentration is positively correlated with OPG concentration and BMD, but inversely correlated with markers of bone turnover [78]. The increase of bone fracture risk in women has been associated with the elevated bone loss observed in the period following menopause (10–15 years) characterised by a rapid decline in oestrogen concentration, an increase in BTM concentrations and a decrease in BMD [128]. Onset of this postmenopausal phase occurs between 50 and 65 years of age (Fig. 6). The higher rate of bone loss (compared to the age-related bone loss) is mainly observed in trabecular bone due to its higher turnover rate and the larger surface area. A recent research however, indicates that cortical bone might also be strongly affected during this phase and characterised by cortical bone trabecularisation [5]. RANKL has been positively correlated with markers of bone turnover, while OPG is negatively correlated with bone turnover [64, 78]. The accelerated phase is then followed by a phase of slow bone loss (Fig. 6).

## 4.2 Risk Factors for Osteoporosis and Osteoporotic Fractures

As highlighted in many reviews, peak bone mass is a major determinant of the risk of osteoporotic fractures [125]. Peak bone mass is usually reached in the third decade of life (Fig. 6) and is strongly governed by environmental factors during growth, with physical activity and nutrition playing major roles. Once the peak is reached, bone mass stays constant until the fourth to fifth decade of life and after that bone loss commences. Due to the fact that women have a lower peak bone mass and an accelerated phase of bone loss due to menopause, bone fracture risk is higher in women compared to men [76]. Peak bone mass and the rate of bone loss during life are influenced by both genetic and environmental factors [173]. These factors include risk factors that can be either non-modifiable or modifiable, such as age, race, sex, life expectancy, menarche, early menopause, family history of OP or fractures, history of fragility fractures, diseases, medications, physical activity, nutritional status, low bodyweight, lifestyle, smoking, excessive consumption of alcohol [74–76, 125, 173]. Bone mass, quality and consequently strength are determined by the combination of these risk factors. In turn, bone strength and the mechanical loading determine the fracture risk. The mechanical load acting on bone can be estimated from either quasi-static loading conditions such as for lumbar spine, or from dynamic loading conditions such as frequency and direction of falls for femoral fractures.

To estimate the individual contribution of genetic and environmental factors on the overall fracture risk is difficult [74, 76]. Considering the complex interactions of these factors in OP, one should distinguish between patient-specific diagnosis of OP and population-specific fracture risk assessment, the latter being a not very accurate measure of fracture risk for an individual [173]. The WHO endorsed a tool named FRAX<sup>®</sup> which takes into account all these risk factors for the prediction of the 10-year risk of osteoporotic fracture in men and women. A link to this tool and other programs that calculate cost effectiveness and quality of life can be found on the website of the *International Osteoporosis Foundation* (<https://www.iofbonehealth.org>). It is worth to mention that FRAX<sup>®</sup> is far from accurate and the development of more sophisticated tools based on bone DSA is required.

## 4.3 Current Diagnosis of Osteoporosis and Whole Bone Strength

BMD is the best single predictor of bone strength, accounting for the 60–85%. Consequently, OP diagnosis is commonly based on BMD measurements [125, 171, 173, 174]. The WHO defined four diagnostic categories for women, based on the T-score evaluation (see Sect. 3.3): (i) *normal* (T-score > -1); (ii) *osteopenia* (-1 < T-score < -2.5); (iii) *osteoporosis* (T-score < -2.5); (iv) *severe osteoporosis* (T-score < -2.5 in the presence of at least 1 osteoporotic fragility fracture) [173].

Nevertheless, these categories are considered arbitrary thresholds strongly dependent on the reference population characteristics, e.g., race and demographics [94].

Despite the strong connection between BMD and bone strength, it is important to recognise that low BMD alone accounts for maximum 44% of the fracture risk [162]. The reason for this is that clinical scientists have exclusively focused on the material side of bone, neglecting entirely the loading conditions. In an attempt to improve the prediction of individual risk of OP and osteoporotic fractures, the BMD value was augmented with other bone material properties contributing to the whole bone strength such as shape, geometry, microarchitecture, bone tissue composition, mineralisation, microdamage and rate of bone turnover. These properties are summarized in the term bone quality [21, 25]. There have been many discussions regarding the suitability of the term bone quality in the context of bone fracture risk assessment. As pointed out by Sievänen and co-workers, bone quality is an imprecise term that should be avoided due to the difficulty of quantitatively include all the factors in a bone strength model and translate their effect into anti-fracture efficacy [156]. It is worth to notice that BMD measurements also contain the mineralisation of bone, consequently it is not possible to separate BMD from bone quality.

More quantitative approaches to estimate bone strength and fracture risk have continuously been developed by the biomechanical community. They result from the combination of 3D micro-CT or HR-pQCT imaging data and multiscale modelling using micromechanical models and finite element (FE) simulations [178]. Based on biomechanical arguments, the concept of bone quality was further discussed. In a review, Hernandez and Keaveny state that, since a bone fracture can be considered a mechanical event, all the clinically relevant modifications of bone quality are likely to affect bone mechanical performance (i.e., strength) relative to bone mass (i.e., BMD) [63]. Based on this consideration, Hernandez proposed a comprehensive hierarchical framework to quantify the biomechanical effect of changes in bone quality parameters at different scales. In particular, this framework was used to investigate how bone turnover could independently influence fracture risk [62].

#### ***4.4 Current and Emerging Treatments***

The aim of OP treatments is to reduce the frequency of bone fractures, especially vertebral and hip fractures which are mainly responsible for morbidity associated with this disease. Different drug treatments can be distinguished according to the following characteristics: mechanisms of action; specific sites and modes of action; route of administration (oral, intravenous, nasal); dosage regimens; degrees of efficacy and effectiveness [13, 32]. Current bone therapeutic guidelines use BMD and BTMs as classification criteria for anabolic and anti-catabolic (previously also referred to as antiresorptive) drugs [131]. According to the terminology of Riggs and Parfitt, anti-catabolic drugs, e.g., bisphosphonates (BPs) and denosumab, act to reduce bone turnover (i.e., reduce bone remodelling) causing an increase in bone strength. These drugs are also associated with a moderately increase of bone mass resulting from

the increased mineralisation of the existing bone matrix. On the other hand, anabolic drugs, e.g., intermittent PTH and sclerostin antibody, strongly increase bone mass by increasing bone remodelling (i.e., high bone turnover) and consequently bone strength. Interestingly, most agents decrease bone resorption (i.e., anti-catabolic treatment), some increase bone formation (i.e., anabolic treatment) and others have been reported to do both [30].

In bone remodelling, osteoblastic and osteoclastic actions are coupled (see Sect. 2.2): osteoblasts are necessary to activate osteoclasts, and osteoclasts secrete factors which stimulate osteoblasts activity. Due to this coupling, anti-catabolic drugs inhibiting bone resorption will also inhibit to a certain extent bone formation. This results in reduced concentrations of bone resorption markers, followed by decreased concentrations of bone formation markers (BP in Fig. 7a). In contrast, anabolic drugs stimulating bone formation will also stimulate bone resorption, resulting in increased concentrations of bone formation markers, followed by increased concentrations of bone resorption markers (PTH in Fig. 7a). The different kinetics driving the changes in bone formation and resorption markers following the anabolic treatment generates a period of time known as the *anabolic window* where bone mass increases. According to this conceptual model, the effect of the anabolic treatment appears to wear off after a certain period of time [12].

The effects on bone microarchitecture of the anti-catabolic treatment with riser-dronate and of the anabolic treatment with teriparatide are illustrated in Fig. 7b. Based on micro-CT imaging data of iliac crest biopsy specimens, treatment with the anti-catabolic agent maintains bone structure, whereas treatment with the anabolic agent promotes bone deposition and both cortical and trabecular thickening. In the following, a brief summary is given on currently available therapies to treat OP together with new emerging strategies, including combined and sequential therapies [45, 55].

### Anti-catabolic Therapies

In clinical practice the most prescribed anti-catabolic drugs are BPs and denosumab. Nitrogen-containing BPs bind to bone surfaces and inhibit the mevalonate pathway in osteoclasts resulting in osteoclast apoptosis. The effects of long-acting BPs such as zoledronate and alendronate can persist for a long time after the end of the treatment [57]. On the other end, denosumab is a fully human monoclonal antibody that binds to RANKL with high affinity and inhibits osteoclast differentiation and activation. The inhibition of osteoclasts ceases within 1 year after discontinuation of the treatment, depending on the dose administrated [102]. Other anti-catabolic drugs commonly used in the treatment of OP are oestrogen, selective oestrogen receptor modulators (SERMs), calcitonin and cathepsin-K inhibitors [45]. Alendronate, riser-dronate, zoledronate and denosumab have a broad spectrum of fracture prevention in patients with OP: the risk of vertebral fractures can decrease by more than 50%, the risk of non-vertebral fractures decreases by 20–25% and the risk of hip fractures decreases by 40–50% [105]. Long-term studies with alendronate and zoledronate indicated a favourable effect on vertebral fractures [9, 148].

During treatments with anti-catabolic drugs the birth of new BMUs is suppressed, resorption cavities become fewer and shallower and bone structure is maintained.

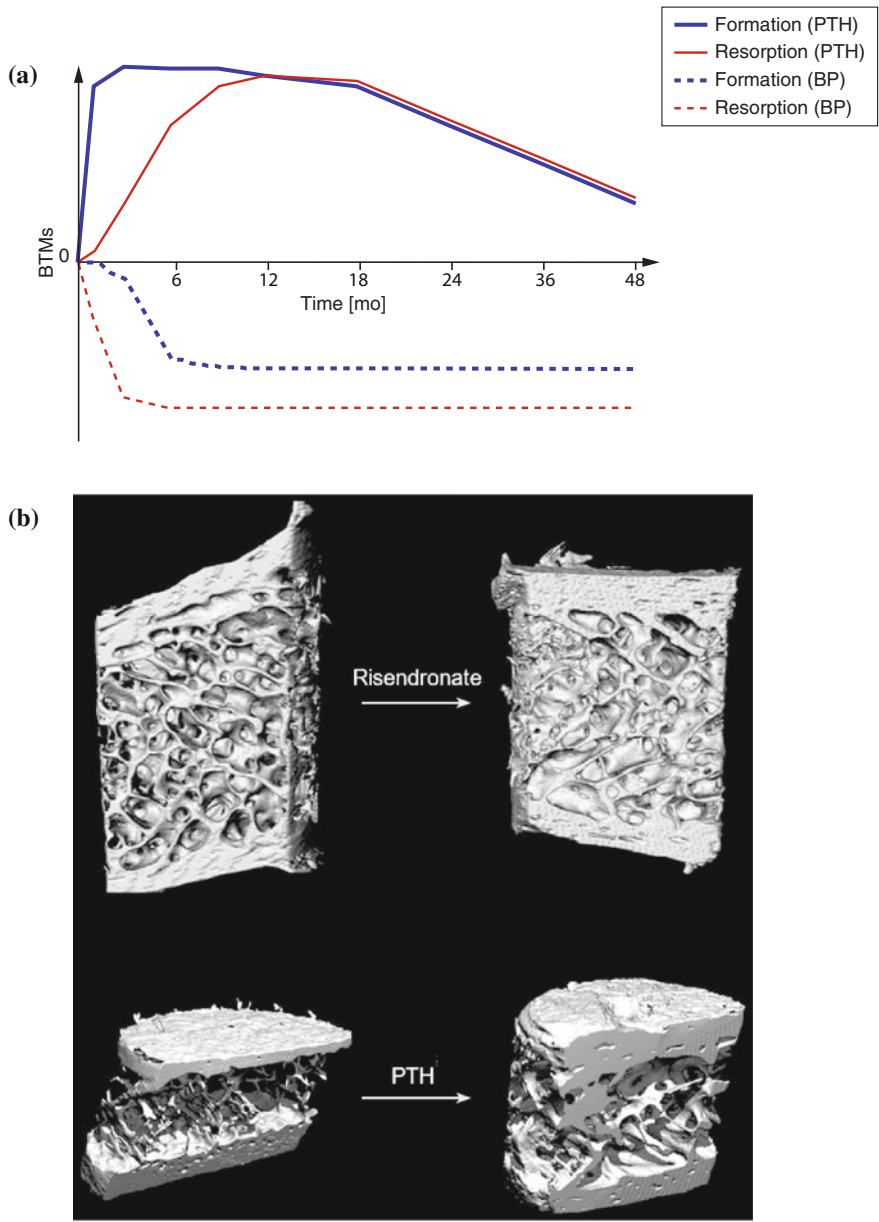


**Fig. 7** Effect of anti-catabolic and anabolic drugs on bone biomarkers: **a** BTMs for PTH (*continuous lines*) and BP (*dashed lines*) treatments. *Thicker curves* indicate bone formation BTMs. *Thinner curves* indicate bone resorption BTMs. **b** Bone microstructural changes of iliac crest biopsy specimens at baseline (*left*) and after 18 months of treatment with risedronate or PTH (*right*), modified from [150]

Moreover, since the remodelling process is slowed down, a more complete mineralisation of the tissue can be obtained: the newly formed bone has time to reach the secondary mineralisation and the older bone keeps mineralising instead of being removed (if remodelling was higher) [98]. As a consequence, bone regions become more homogeneous. Based on the fact that changes in BMD plateau after a rather long period of time (approximately 2–3 years), it seems that secondary mineralisation may be a good candidate to explain the increase in BMD.

### **Anabolic Therapies**

Physiological exercise and related mechanical stimuli can act as anabolic agents on bone [114]. Large intense challenges to the skeleton, as well as brief exposure to mechanical signals of high frequency and low intensity, have been shown to provide a significant anabolic stimulus to bone. Physical activity has been proven to have a positive effect on building peak bone mass and density [111]. It directly affects osteoblast and osteocyte activities, but can also bias mesenchymal stem cell differentiation towards osteoblastogenesis instead of adipogenesis [114]. This fact in particular indicates that, at least during growth, physical activity targets bone marrow stem cells, hence, it might be considered as a novel drug-free anabolic therapy.

Currently, the only anabolic drug available is teriparatide, a recombinant 1–34 N-terminal fragment of endogenous human PTH [rhPTH(1–34)]. In patients with severe OP, daily subcutaneous injections of teriparatide during 18 months decreased the risk of vertebral fractures by 65% and the risk of non-vertebral fractures by 53% [92, 110]. The mechanisms behind the increased bone formation driven by the intermittent administration of PTH (i.e., daily injection of the drug) are still not fully understood. The overall action of the treatment is to increase osteoblast differentiation and proliferation, while reducing osteoblast apoptosis. In trabecular bone, teriparatide increases BMD and trabecular thickness [73]. In cortical bone, teriparatide increases endosteal bone remodelling and periosteal bone formation [20]. These results indicate that teriparatide has an effect on both bone modelling and remodelling [6]. The duration of a treatment with teriparatide is generally between 18 and 24 months and the action of the drug is believed to be maximally anabolic during the anabolic window (as mentioned above). After 18–24 months of treatment, bone resorption appears to catch up with bone formation and the newly formed and lowly mineralised bone is quickly lost [6, 12]. To preserve the new bone and allow further mineralisation, the established treatment protocol requires the administration of an anti-catabolic drug at the cessation of the treatment with teriparatide.

In animal studies, the use of anti-sclerostin monoclonal antibodies appears to directly stimulate bone formation via bone modelling, i.e., at least partially independent of the activation frequency and bone remodelling [6]. In addition, these antibodies stimulated the production of OPG resulting in decreased bone resorption and leading to the uncoupling of bone formation and bone resorption processes. Potentially, the use of sclerostin antibodies could result in an even greater anabolic window compared to teriparatide. Subcutaneous injections of the anti-sclerostin antibody romosozumab have been studied in phase I and II trials [99, 115]. In postmenopausal women with low bone mass, a 12-month treatment with a monthly dose of 210 mg of

romosozumab was associated with a significant increase in BMD (11.3% at the spine, 4.1% total hip and 3.7% at the femoral neck) greater than the ones obtained with weekly alendronate or daily teriparatide treatments. There was a transient increase in bone formation markers during the first 3 months together with an initial 2-month decrease in bone resorption markers, which was to a lesser degree sustained during the 12 months.

### Combined Therapies

Despite the development of new therapeutic treatments for OP in the past decades, the currently approved drugs are not able to restore normal bone integrity in the majority of osteoporotic patients. To increase the therapeutic efficacy, latest OP treatments combine anabolic and anti-catabolic drugs. Clinical trials showed that the effect of the combined therapy on BMD depends on the timing of the anabolic drug administration (i.e., before, during or after the administration of the anti-catabolic drug), on the specific drugs used and on the particular bone site analysed [34, 46]. The most consistent effect of the combined therapy is a greater BMD increase at the hip compared to the treatment with the anabolic agent alone, in particular when teriparatide is associated with BPs or denosumab [34]. On the contrary, no benefit of the combined therapy has been shown on the BMD at the spine. In patients treated with BPs only and who still develop bone fractures or loose BMD, switching to a treatment with teriparatide is advocated. In addition, the continuation of the anti-catabolic treatment when starting the teriparatide one resulted in a better response of the BMD at the hip [35]. On the other hand, an anti-catabolic treatment is indicated after stopping the administration of teriparatide in order to preserve the increased bone architecture and enhance its mineralisation.

In conclusion, the site and the mode of action of a particular treatment depend on the PK properties of the specific drug (or combination of drugs) and the underlying bone pathology of the single individual. Consequently, the duration of the effects on BTMs and BMD after the withdrawal of a treatment can be different, perhaps indicative of disease modification or at least suggesting an appropriate treatment duration [125]. In order to compare treatments on a common basis, conceptual and mathematical models describing these combined dynamics can play a crucial role. Progresses in development of such models are given in the next sections.

## 5 Basics of Disease System Analysis

### 5.1 PK/PD Modelling

The development of PK/PD models in the last 20 years has had as primary objective the characterisation of the drug effect over time, then used to optimise dosing regimen and delivery profile of both new and existing drugs. Recently, PK/PD models have also been applied during the drug development process [41, 124]. To clarify the

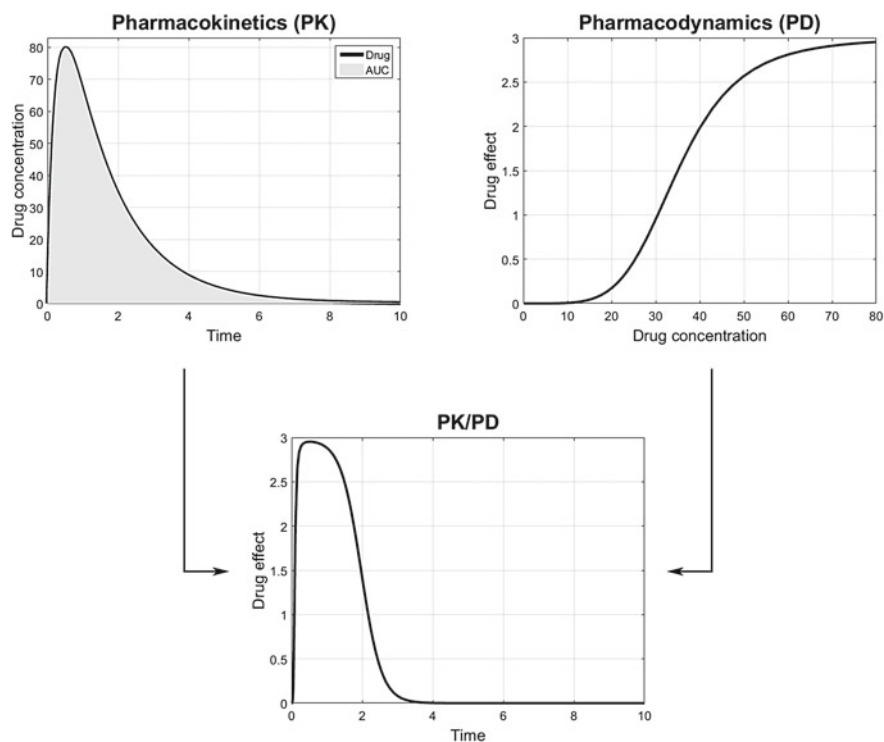


**Fig. 8** Combination of a PK model and a PD model in the PK/PD modelling process (AUC indicates the area under the curve)

difference between pharmacokinetics and pharmacodynamics, Holford and Sheiner came up with these simple and practical definitions: pharmacokinetics is *what the body does to the drug*, whereas pharmacodynamics defines *what the drug does to the body* [66]. A PK model is a mathematical description of the change over time of the drug concentration in the body fluid (i.e., blood, plasma or serum)<sup>2</sup> after the administration of a certain drug dose. PK models are used to simulate the rate of drug absorption, distribution and elimination in order to describe and predict the drug concentration in the body over time. A PD model, on the other end, describes the intensity of the drug effect relative to its concentration in the body fluid. The combination of a PK model and a PD model is known as PK/PD model of the drug (Fig. 8) and allows the description of the drug effect over time [100].

A common tool used to describe the pharmacokinetics of a drug is the *compartment-based* PK model [154]. According to this model, the drug is assumed to enter, distribute and leave an hypothetical compartment containing a volume of

<sup>2</sup>It is important to distinguish between blood, plasma, and serum. Blood includes fluid, white and red cells and platelets; plasma is the fluid portion of blood including only soluble proteins; serum is the plasma without the soluble protein.

fluid that equilibrates with the drug. This compartment is not an anatomical structure, but it represents a group of tissues with similar blood flow and drug affinity, balancing with the drug in an uniform way. In the one-compartment open model, the drug is added to and eliminated from a single compartment, also denoted as *central compartment*, which represents the plasma and the highly perfused tissues. In the two-compartment open model, the central compartment communicates with a second compartment (*tissue compartment*) and the drug disposition is related to the exchange between the two. The one-compartment open model for an intravenous injection (IV bolus) is the simplest mathematical way to describe the process of drug distribution and elimination. In this model the drug is assumed to be injected all at once, the distribution is assumed instantaneous and homogeneous throughout the central compartment and the drug elimination starts immediately after the injection.

To describe the change over time of the drug concentration in the compartment following the injection of a certain dose, two primary PK parameters need to be considered: the *volume of distribution* of the compartment and the *clearance* of the drug [154]. The volume of distribution is a proportionality factor that correlates the amount of drug in the body to the drug concentration measured in the biological fluid. Although it has the dimension of a volume, it is not a physiological measurable quantity, hence, it is often referred to as *apparent* volume of distribution. The volume of distribution is linked to the dose of drug administered and to the plasma drug concentration immediately after the dose injection by means of the following equation:

$$D = V_D \cdot C_p, \quad (1)$$

where  $D$  is the drug dose expressed in mg,  $V_D$  is the volume of distribution in  $\text{mm}^3$  and  $C_p$  is the plasma drug concentration in  $\text{mg}/\text{mm}^3$ . A drug dose is generally proportional to the volume of distribution, i.e., the larger the volume of distribution, the larger the dose has to be to achieve the target concentration. In an adult, approximately 60% of the total body weight is water, made up of intracellular fluid (35%) and extracellular fluid (25%). The extracellular fluid includes plasma (4%) and the interstitial fluid surrounding the cells outside the vascular system (21%). According to this partition, low  $V_D$  indicates that the drug is distributed only in the extracellular fluid. If  $V_D$  is close to the total body water ( $\approx 40$  l), the drug distribution involves the total body water. When  $V_D$  is larger than the total body water, the drug is probably concentrated in the tissues outside the plasma and in the interstitial fluid, consequently resulting in a low plasma concentration.

The concentration of the drug is also regulated by the amount of drug eliminated per unit of time (*elimination rate*). For most drugs, the elimination process is assumed to be a *first order reaction* [154], meaning that the elimination rate is directly proportional to the amount of drug present in the system (Eqs. (2) and (4)). For other drugs instead, the amount of drug is assumed to decrease at a constant rate and the elimination process is defined as *zero-order reaction*. When considering a first order reaction we can describe the elimination process as follows:

$$\frac{dD}{dt} = -k \cdot D, \quad (2)$$

where  $\frac{dD}{dt}$  is the elimination rate expressed in mg/h and  $k$  is the *first order elimination rate constant*. Integrating Eq. (2) we obtain the expression of the change over time of the amount of drug in the body:

$$D = D_0 \cdot e^{-k \cdot t}, \quad (3)$$

where  $D_0$  is the initial drug dose. The same considerations can be done expressing Eqs. (2) and (3) in terms of drug concentration:

$$\frac{dC_p}{dt} = -k \cdot C_p, \quad (4)$$

$$C_p = C_{p0} \cdot e^{-k \cdot t}, \quad (5)$$

where  $C_p$  is the concentration of the drug in  $\mu\text{g/ml}$ . The time required for a certain drug concentration to decrease by one half is a characteristic parameter of the drug pharmacokinetics defined as drug *half-life*. It is generally expressed in h and in case of first order elimination is constant and equal to:

$$t_{1/2} = \frac{0.693}{k}, \quad (6)$$

where  $t_{1/2}$  indicates the half life.

Drug clearance is another fundamental parameter used to describe the drug elimination process in pharmacokinetics. It is defined as the volume of either plasma or blood cleared from the drug per unit of time. Clearance is measured in ml/h and consists of a constant parameter related to the volume of distribution and to the elimination rate constant as follows:

$$CL = k \cdot V_D, \quad (7)$$

where  $CL$  is the clearance.

When the drug is not administered intravenously (e.g., oral administration or subcutaneous injection), the PK model needs also to account for the *absorption process* of the drug from the site of administration into the plasma, and for the *bioavailability* of the drug in the systemic circulation. For such cases, additional pharmacokinetics parameters are necessary (see also example of OP treatment with denosumab in Sect. 6.1). Most PK models for extra-vascular drug administration consider the absorption process as a first order reaction. As for the elimination process, the absorption of the drug is described via a rate constant. Drug absorption is usually faster than its elimination. It is important to mention that the elimination process begins as soon as the drug enters the plasma and starts to be distributed in all tissues, even if the absorption process is not complete. During the absorption phase, the rate of drug

absorption is greater than the rate of drug elimination. When the plasma drug concentration reaches its peak, the rate of drug elimination equals the rate of drug absorption (i.e., the amount of drug in the body does not change). In the post-absorption phase, the elimination rate is higher than the absorption rate. As soon as the amount of drug at the absorption site is null, the absorption rate equals zero and the system is described by the elimination phase only.

The actual exposure of the body to the drug, following the administration of a certain dose, can be quantified measuring the *area under the curve* (AUC) of the *plasma concentration versus time* curve (Fig. 8). During clinical trials, the plasma, blood or serum drug concentration in a patient can be measured at several time points and used to create a patient specific profile of the drug concentration change over time. From this profile AUC can be estimated. Mathematically, AUC is defined as the integral of the drug concentration versus time curve and is generally expressed in  $\mu\text{g}\cdot\text{h}/\text{ml}$ . It depends on the drug elimination and absorption rates and the administered dose. For drugs following linear kinetics, AUC is directly proportional to the dose and inversely proportional to the clearance. In particular, the higher the clearance, the shorter the time that the drug spends in the systemic circulation and the faster the reduction of the drug concentration. Consequently, the exposure of the body to the drug is shorter and AUC is smaller. Therefore, AUC is related to the amount of drug absorbed in the systemic circulation.

Following an intravenous injection, the dose administered is assumed to entirely enter the systemic circulation in an active form. In case of extra-vascular administration instead, only a part of the entire dose reaches the systemic circulation in an active form. Following this considerations, AUC can be used to define another important PK parameter: the drug bioavailability. This parameter represents the fraction of the administered dose that enters the system circulation in an active form. By definition, a drug administered intravenously has bioavailability equal to 100 %, therefore it is used as reference for the computation of the bioavailability of a drug following an extra-vascular administration. Numerically, the bioavailability of a certain dose of a specific drug is computed as the ratio between AUC corresponding to an extra-vascular administration and AUC corresponding to an intravenous administration. Often, volume of distribution and clearance are given as function of the bioavailability.

Taking into account absorption, elimination and bioavailability of the drug, the rate of drug variation in the body and the drug concentration can be expressed as follows:

$$\frac{dD}{dt} = \text{rate}_{in} - \text{rate}_{out} = F \cdot k_a \cdot D_0 \cdot e^{-k_a \cdot t} - k \cdot D, \quad (8)$$

$$C_p = \frac{F}{V_D} \cdot \frac{k_a \cdot D_0}{(k_a - k)} \cdot (e^{-k \cdot t} - e^{-k_a \cdot t}), \quad (9)$$

where  $F$  is the bioavailability,  $k_a$  is the absorption rate constant expressed in  $1/\text{h}$  and  $\frac{F}{V_D}$  is the inverse of the volume of distribution given as a function of the bioavailability. As previously mentioned, at the peak plasma concentration the rate of drug absorption

equals the rate of drug elimination. This assumption allows the computation of the *peak time*, i.e., the time required to reach the peak drug concentration:

$$t_{max} = \frac{\ln(k_a/k)}{k_a - k}, \quad (10)$$

where  $t_{max}$  indicates the peak time, generally expressed in h. Note that the peak time is a parameter of the drug independent of the administered dose.

Once the mathematical description of the drug concentration time course in the body fluid is completed, a PD analysis is used to quantify the relationship between the drug concentration and its effect. Ideally, the drug concentration should be measured at the effect site (i.e., site where the drug interacts with its receptor), in case of OP for example it should be at the interested bone site. Since this is generally not possible, it is common practise to use either the plasma or the blood drug concentration and to assume that, under PK steady-state conditions, the concentration in plasma or blood is in equilibrium with the pharmacologically active, unbound, drug concentration at the effect site [100]. The effect of the drug can be evaluated measuring the variation of physiological parameters. In OP for example, changes in the bone resorption and formation activities are monitored. Several PD models have been developed so far, such as fixed effect, linear, log-linear,  $E_{max}$  and *sigmoid*  $E_{max}$  models. Among these, the  $E_{max}$  and the *sigmoid*  $E_{max}$  are the most commonly used (Fig. 8). In the  $E_{max}$  model, the effect of the drug is expressed as function of the *intrinsic activity* of the drug (i.e., maximum effect possible) and the *potency* of the drug (i.e., concentration that causes 50% of the intrinsic activity) [100, 154]:

$$E = E_0 \pm \frac{E_{max} \cdot C}{E_{50} + C}, \quad (11)$$

where  $C$  is the drug concentration,  $E_{max}$  is the intrinsic activity,  $E_{50}$  is the potency and  $E_0$  is the baseline effect existing in the absence of the drug. The latter can be either stimulated (+) or inhibited (−) by the drug effect.  $E_0$  is assumed equal to zero (i.e., in the absence of the drug the effect is null) when the receptor theory is applied to the equilibrium interaction of the drug with the site of action. The  $E_{max}$  model describes two key features of the pharmacologic response: (i) the hyperbolic pharmacologic response versus drug concentration curve, and (ii) the max response induced by a certain drug concentration beyond which no more increase in the response is obtained. The sigmoid  $E_{max}$  model is an extension of the  $E_{max}$  model describing the pharmacologic response versus drug concentration curve for s-shaped rather than hyperbolic drugs. The effect is calculated as:

$$E = E_0 \pm \frac{E_{max} \cdot C^n}{E_{50}^n + C^n}, \quad (12)$$

with  $n$  being a parameter denoting the steepness of the curve. Theoretically,  $n$  should be related to the number of drug molecules that combine with each receptor, however,

it is mainly used as a phenomenological factor that allows a good fit of the experimental data. The larger  $n$ , the steeper the linear phase of the plasma concentration (log) versus effect curve [100, 154].

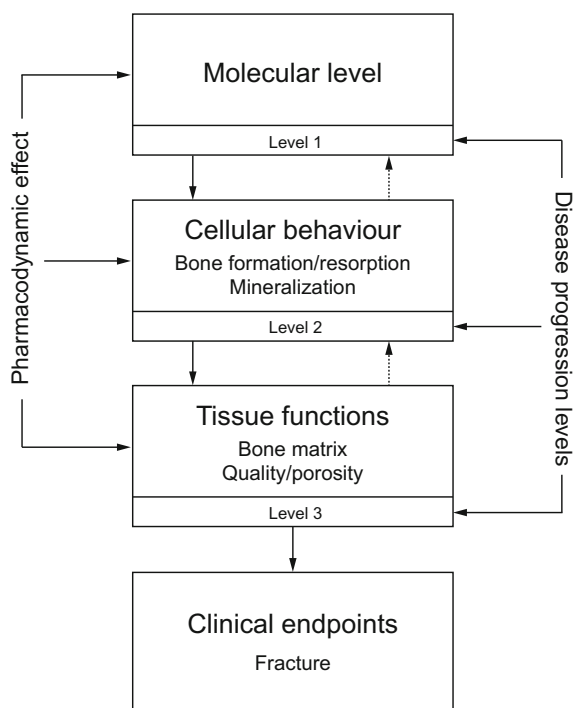
The conventional PK/PD models described so far are characterised by a descriptive approach which is empirical and driven by a large amount of data. As a consequence, they cannot predict a clinical response beyond the data which they are based on. To overcome this limitation, more sophisticated models have been developed which take into account both the underlying mechanisms of the disease and the drug action [41, 126, 147]. They are referred to as *mechanism-based* or *mechanistic* PK/PD models and aim to characterise the intermediate processes between the drug administration and its effect, relying on biomarker data such as receptor binding and activation and feedback pathways. There are two types of parameters used to describe these models: the ones describing the properties of the drug (e.g., affinity and target activation) and the ones describing the properties of the biological system [41, 124]. In the context of mechanism-based PK/PD modelling, the sequence of events following the activation induced by the drug and governing the in vivo pharmacological response is referred to as *transduction*. This process is generally non-linear and can either be fast (rate constants between milliseconds and seconds) or slow (rate constants in the order of hours to days). In the first case, since the rate constants controlling the disposition of the drug are typically between minutes and hours, the transduction does not cause a delay in the pharmacological effect. In the second case instead, it becomes a fundamental parameter in the definition of the drug action over time [41, 124].

## 5.2 Disease Progression Analysis

Another limitation of the conventional PK/PD analysis worth to mention is the representation of the system baseline using constant parameters (e.g.,  $E_0$  in Eqs. (11) and (12)). In case of degenerative diseases such as OP, Alzheimer's disease, Parkinson's disease, sarcopenia and osteoarthritis, this approach is not realistic because the biological functions deteriorate over time due to slow changes in the disease status. To take into account the changes in the system due to the progression of the disease, mechanism-based PK/PD models also include a *disease progression analysis* [29, 65, 124]. Furthermore, the use of disease progression models is fundamental when drug treatments specifically aim to modify the progression of the disease [41]. In particular, clinical pharmacology can be described in terms of *disease progression*, i.e. changes in the disease status over time, and *drug action*, i.e. the effect of the drug on the disease progression [29]. Disease progression can be analysed at different levels of the pathophysiology (Fig. 9) [124]. Bone healthy remodelling state, for example, can initially be perturbed at the molecular level (level 1) where the interactions between genetic and transcription events and receptor-ligand binding reactions take place. The result of these molecular changes may affect the behaviour of bone cells regulating bone resorption and bone formation events (level 2). These changes

**Fig. 9** DSA in OP:

individual levels represent stages of bone disease. Bone biological function within the homeostatic state of remodelling may be disturbed at level 1 or 2, resulting in an imbalance of bone resorption and bone formation. This imbalance can be observed at the bone tissue level (level 3) as an increase in porosity and/or variation in bone quality. At the clinical endpoint, these changes may result in bone fractures. The 3 stages of the disease specifically represent the combined outcome of disease progression and pharmacodynamic effect



in turn regulate bone tissue properties such as porosity and bone quality (level 3). At the clinical endpoint these changes may eventually result in bone fractures. At each of the mentioned levels, disease progression and pharmacodynamic effect are combined to produce a certain outcome on the disease over time behaviour. The level at which the disease behaviour is described in the disease progression analysis, depends on the information available.

In ageing, the natural progression of the disease involves phenomena such as cell death and loss of organ functions. An interesting aspect worth to investigate is whether the development of degenerative diseases is exclusively driven by ageing or if other factors are also involved. From a statistical prospective, the occurrence of degenerative diseases appears to be mainly age-related. However, ageing alone cannot explain the different disease progression pattern and the faster rate of cell loss found in patients with either Alzheimer's or Parkinson's disease [29].

### Aims of Drug Treatments

Drug treatments aim to either reduce, stop or reverse the natural process of a disease. According to the way in which the drug affects the disease status, its effect can be defined either *symptomatic* or *protective*. A symptomatic treatment effect improves the severity of the symptoms without modifying the disease progression. A protective treatment effect, on the other hand, involves a modification of the underlying disease progression leading to an improved disease status. A combination of both

symptomatic and protective effects is also possible. In general, symptomatic effect action is faster compared to the protective effect one. A review of several disease progression models based on clinical endpoints is provided by Chan and Holford for diseases such as Parkinson's, Alzheimer's, and OP [29].

Similarly to the use of drug concentration in a PK model and drug effect in a PD model, the disease status is used in a disease progression model to identify the disease pathway [65]. A simple disease progression model can be described with the following equation:

$$S(t) = S_0 + \frac{E_{max} \cdot C_e(t)}{E_{50} + C_e(t)}, \quad (13)$$

where, similarly to Eq. (11),  $S(t)$  is the time course of the disease status determined by both the underlying disease and the drug action,  $S_0$  refers to the baseline disease status and  $C_e$  is the drug concentration at the effect site [65]. The downside of this model is that it does not account for a time course of the disease status independent of the drug effect. Even though it could be reasonable to use this model when the observation time is short, however, modelling the changes of the disease status over time independently of the drug effect is necessary. From this prospective, Chan and colleagues [29] and Holford and co-authors [65] proposed two models of natural disease progression (i.e., without the drug effect on the disease progression), one linear and one asymptotic. The linear model is expressed as follows:

$$S(t) = S_0 + \alpha \cdot t, \quad (14)$$

where the rate of disease progression is linear with a constant slope defined by the parameter  $\alpha$ . In the asymptotic model on the other hand, the worsening of the disease status is considered exponential and approaching to a steady state as follows:

$$S(t) = S_0 \cdot e^{-\frac{\ln(2) \cdot t}{TP}} + S_{ss} \cdot \left[ 1 - e^{-\frac{\ln(2) \cdot t}{TP}} \right], \quad (15)$$

where  $TP$  indicates the half-life of the drug and  $S_{ss}$  is the maximum burnt-out disease status. The natural disease progression curves for the linear and the asymptotic models are shown as black solid lines in Fig. 10a, b respectively.

According to the type of treatment simulated (i.e., symptomatic or protective), model parameters reflecting the action of the drug are conveniently modified. In particular, in the case of a symptomatic drug effect, the parameters describing the underlying disease progression (i.e.,  $\alpha$  in the linear model,  $TP$  and  $S_{ss}$  in the asymptotic model) do not change. Consequently, the symptomatic effect is generally included in the disease progression model as an additive term. In a linear model for example we can have:

$$S(t) = S_0 + \alpha \cdot t + E(t), \quad (16)$$

where  $E(t)$  represents the symptomatic effect. Assuming that this effect is constant for a given time interval, one can observe a constant offset from the natural disease

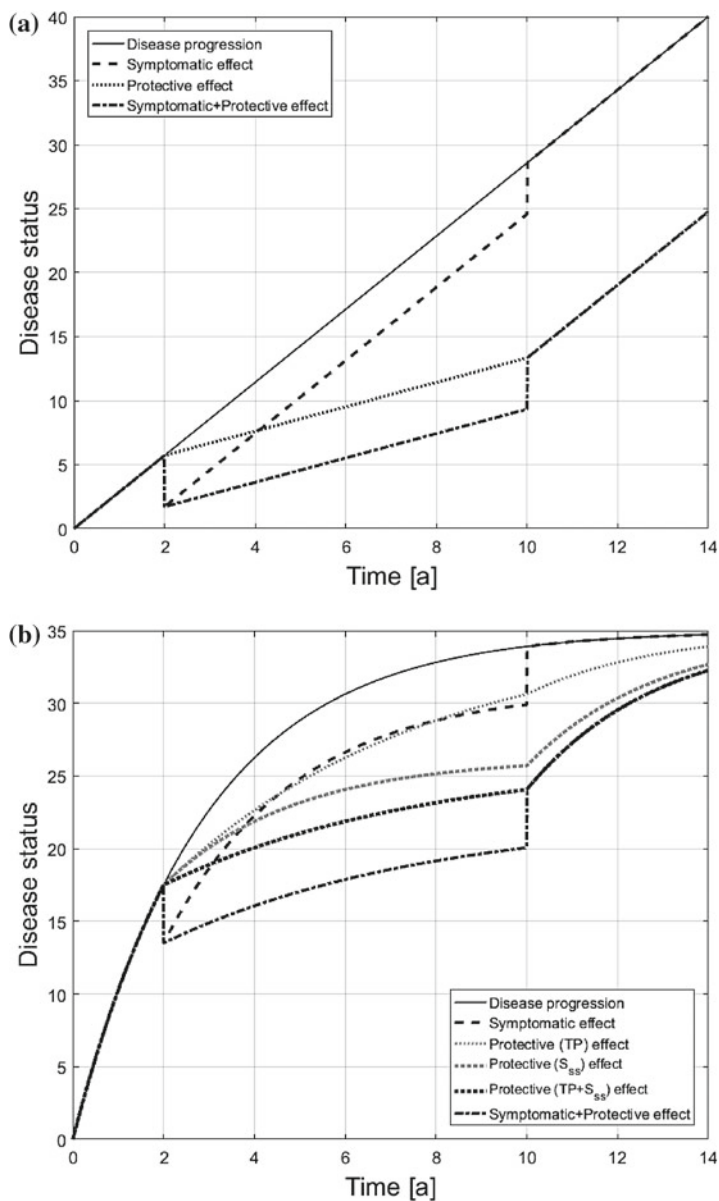


**Fig. 10** Disease progression and drug intervention models: disease status versus time for a linear model (a) and an asymptotic model (b). *Black solid curves* represent the disease progression without drug intervention, *black dashed curves* represent the symptomatic treatment effect, *black dot curves* represent the protective treatment effect, *black dash-dot curves* represent the combined symptomatic and protective treatment effect. *Gray dot curves* in (b) represent the  $TP$  protective treatment effect (light) and the  $S_{ss}$  protective treatment effect (thick) separately

progression (dashed black curves in Fig. 10a, b) indicating a delay in the time needed by the disease to reach the same status as at the start of the treatment. When the treatment is stopped, the natural disease progression pattern is followed.

In the case of protective effect, the action of the drug influences the rate of disease progression and it is described as a change in the slope of the disease progression curve. In a linear model it follows that:

$$S(t) = S_0 + [\alpha + E(t)] \cdot t, \quad (17)$$

where  $E(t)$  represents the protective effect. Assuming that this effect is constant for a given time interval, the effect of the drug action on the disease status is shown in the dotted curves in Fig. 10a, b. When an asymptotic model is used, the protective effect can act either on  $TP$ , resulting in a change of the curvature of the natural disease progress model (see grey light dotted curve in Fig. 10b), on  $S_{ss}$  (see grey thick dotted curve in Fig. 10b) or on both (see black dotted curve in Fig. 10b). The protective effect is shown in Fig. 10a, b as the difference between the untreated disease status curve (black solid line) and the treated one (dotted line) at the end of the treatment, when the rate of disease progression returns to the natural value, indicating that the treatment benefit continues also after drug effects have ceased.

Sometimes the ability to distinguish between symptomatic and protective effects can be challenging and both the effects may occur together. In this case, the total effect is defined as *symptomatic + protective* and, in a linear model for example, can be described with an additive term and a change of the slope of the disease progression model:

$$S(t) = S_0 + E_0(t) + [\alpha + E_s(t)] \cdot t, \quad (18)$$

where  $E_0(t)$  is the additive term and  $E_s(t)$  is the change in the slope. Assuming that these two variables are constant for a given time interval, the combined symptomatic + protective effect of the drug results in the dash-dot curves in Fig. 10a, b.

### Disease Progression Model of Postmenopausal Osteoporosis

The disease progression models described above are here applied to PMO, together with symptomatic and protective effects acting on the disease progression to either reduce or slow down the bone loss. As already mentioned in Sect. 3, BMD and BV/TV are the clinical parameters most commonly monitored in OP patients. In general, BMD in OP decreases over time (Fig. 6). In particular, PMO in women induces a BMD decline at a rate of up to 2%/yr. As previously pointed out, the loss of BMD is largely linked to the increase in bone porosity, for this reason, either BMD, BV/TV or porosity itself can be used as parameters describing the disease status. Assuming a linear disease progression model, the BMD variation over time in PMO is reported in Fig. 11. The dashed curves represent the natural PMO progression, whereas symptomatic, protective and combined treatment effects are shown as solid lines in the top, middle and bottom panels respectively. It is worth to notice that comparing the natural disease progression curve reported in Fig. 11 with the

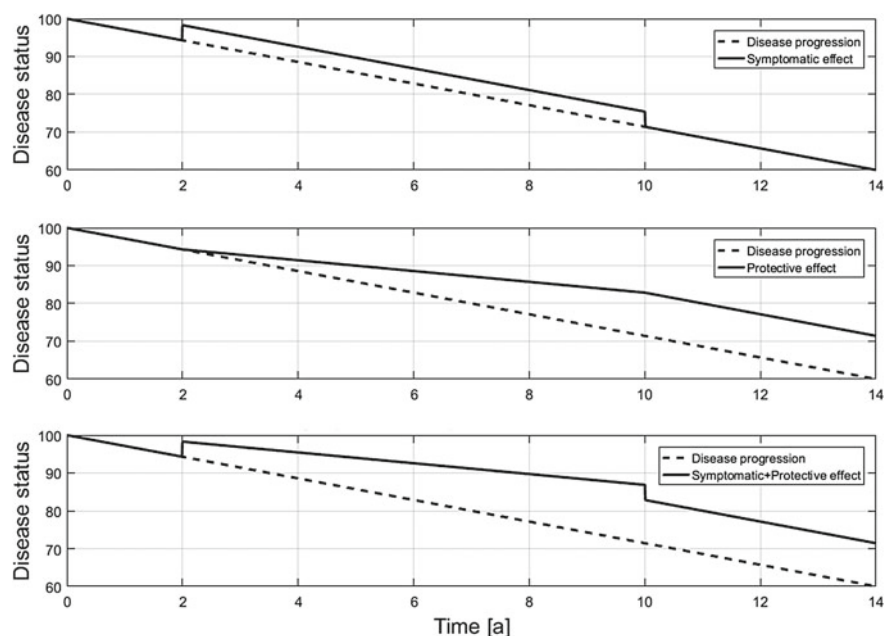


**Fig. 11** Disease progression and drug intervention in PMO: PMO status (e.g., BMD change) versus time in a linear model. *Dashed curves* represent the disease progression without drug intervention. *Solid curves* represent respectively symptomatic (*top panel*), protective (*middle panel*) and combined symptomatic + protective (*bottom panel*) treatment effects

schematic curve representing PMO in Fig. 6, it is evident that the change in bone loss rate is not well represented with a linear model. A piecewise linear model in fact, would represent more realistically the non-linear disease progression. On the other hand, assuming an asymptotic disease progression model, the BMD variation over time is represented in Fig. 12. The dashed curves represent the natural PMO progression, whereas the treatment effects are shown as solid lines. The asymptotic model is able to well represent the non-linear natural disease progression of PMO, which is characterised by a rapid BMD reduction in the first 5 years of the disease followed by a relatively linear progression thereafter. A symptomatic effect is shown in the top panel of Fig. 12a, whereas different protective effects are shown in the middle and bottom panels of Fig. 12a and in the top panel of Fig. 12b. The bottom panel of Fig. 12b shows a combined treatment effect. Due to the slow changes in BMD over time, however, it is not clear how to estimate when the full treatment effect is reached and how to distinguish between protective and symptomatic effects.

All the cases discussed so far assumed a drug effect acting instantaneously on the disease progression. A more consistent way to represent the action of a drug on the disease status is to take into account the time required for a drug to exert its effect (*wash-in*) and the time required for the drug to lose its effect (*wash-out*) [65]. In more detail, the drug wash-in represents the time delay between the starting point of the treatment and the achievement of a constant drug action. This delay might be

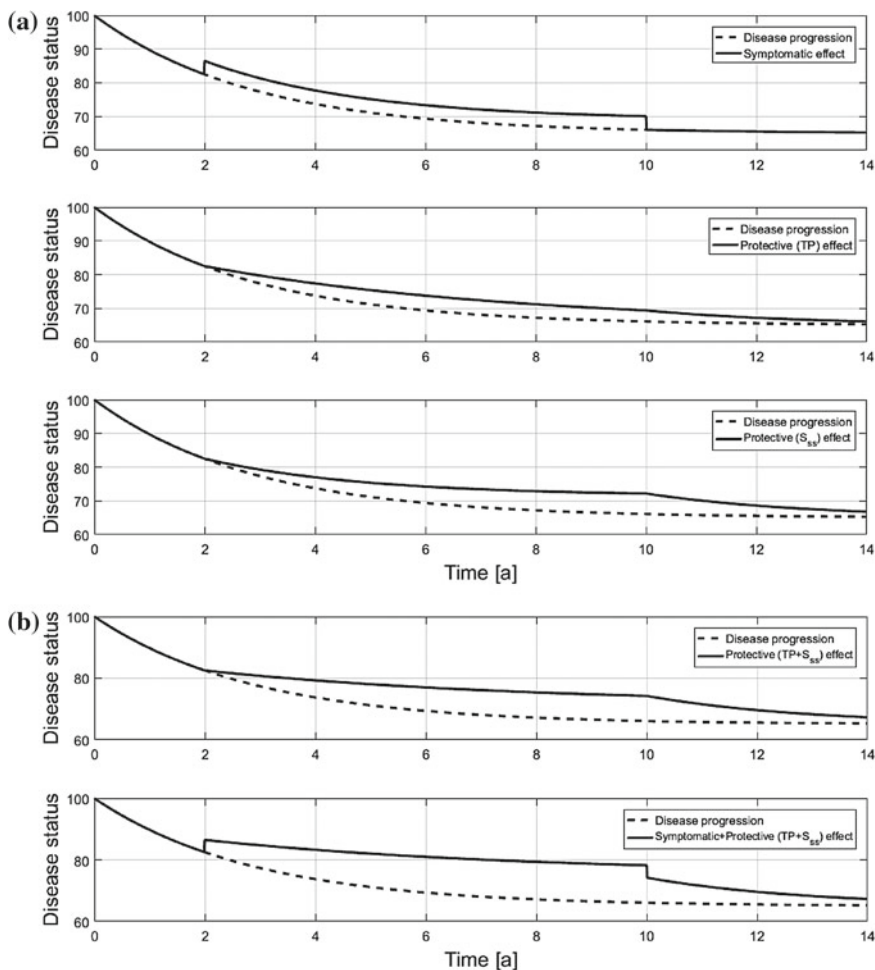


**Fig. 12** Disease progression and drug intervention in PMO: PMO status (e.g., BMD change) versus time in an asymptotic model. *Dashed curves* represent the disease progression without drug intervention. *Solid curves* represent respectively symptomatic treatment effect ((a), *top panel*), protective treatment effect acting on  $TP$  ((a), *middle panel*), protective treatment effect acting on  $S_{ss}$  ((a), *bottom panel*), combined protective treatment effect  $TP + S_{ss}$  ((b), *top panel*), combined symptomatic + protective  $TP + S_{ss}$  treatment effect ((b), *bottom panel*)

due to the drug absorption process, to its distribution to the effect site and to binding reactions with its receptors. On the other hand, the drug wash-out is the time needed to completely remove the drug effect after the withdrawal of the treatment. The BMD change over time in a linear disease progression model taking into account also the wash-in and the wash-out of the drug are reported in Fig. 13. The dashed curves represent the natural PMO progression model, whereas symptomatic, protective and combined treatment effects are shown as solid lines in the top, middle and bottom panels respectively.

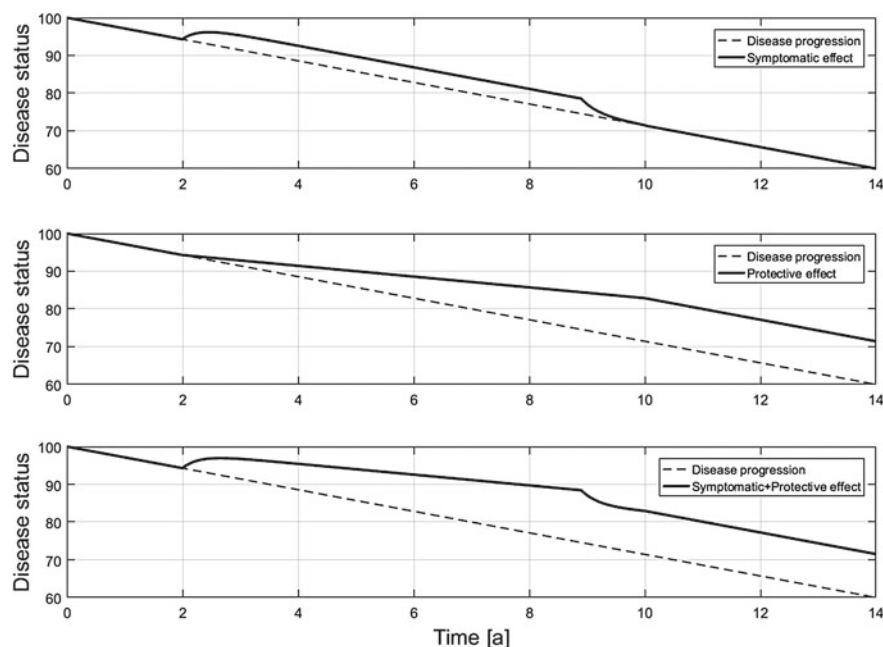


**Fig. 13** Disease progression and drug intervention in PMO: PMO status (e.g., BMD change) versus time in a linear model taking into account the time required for the drug to exert its effect (wash-in) and for losing its effect (wash-out). *Dashed lines* represent the disease progression without drug intervention, *solid curves* represent respectively symptomatic (*top panel*), protective (*middle panel*) and combined symptomatic + protective (*bottom panel*) treatment effects

## 6 Disease System Analysis of Osteoporosis

As introduced in Sect. 5.1, mechanistic PK/PD models use specific expressions to characterise pharmacokinetics and mechanism of action of a drug, as well as physiological processes. A feature specific to this type of models is the differentiation between drug-specific and system-specific parameters. In Sect. 5.2, PMO and the associated bone remodelling process were described via linear and asymptotic disease progression models in which all the details of the underlying molecular actions were lumped into phenomenological parameters describing, for example, the rate of bone loss. In this section, we will formulate a mechanistic model of the bone remodelling process that takes into account the major molecular regulatory pathways. Successively, we will apply this mechanism-based disease progression model to the analysis of PMO progression and its treatment with the anti-catabolic drug denosumab. In this regard, we will closely follow the approach taken by Scheiner and co-workers [146].

A PK model of denosumab has been developed based on the experimental data from Bekker et al. [10] and used to predict blood serum concentrations of the drug

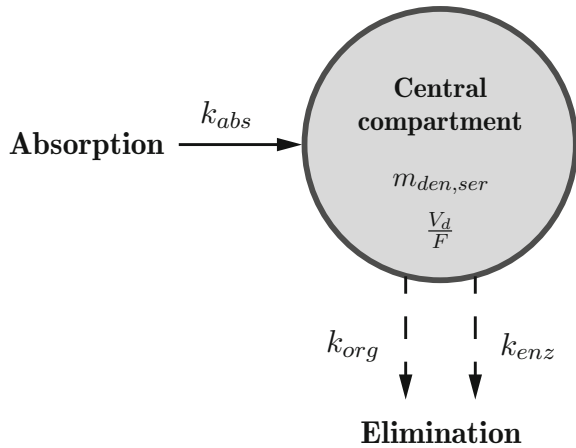
after subcutaneous administration of different doses (see Sect. 6.1). Subsequently, this PK model has been linked to the mechanobiological model of bone remodelling developed by Pivonka and co-workers [121, 122, 145] which takes into account key features of the known physiology of bone remodelling, including the most significant biochemical and biomechanical regulatory mechanisms (see Sect. 6.2). This mechanobiological model allowed the simulation of disease progression in PMO based on molecular and cellular mechanisms. The time-dependent increase of RANKL expression together with the decreased mechanosensitivity of osteocytes have been included in the model to accurately reflect the disease progression in PMO (see Sect. 6.3). Furthermore, this model allowed the introduction of the PD effect of the drug in different points of action, such as cell differentiation, proliferation and apoptosis. In particular, the action of denosumab has been incorporated in the RANK-RANKL-OPG pathway according to the receptor-ligand binding reaction theory (see Sect. 6.4). Eventually, this mechanistic model has been used to simulate PMO with and without the administration of denosumab. The results obtained were investigated and compared with experimental biomarker data (BMD and BTMs) from the literature (see Sect. 6.5).

## 6.1 Denosumab PK Model

As previously mentioned, denosumab is a fully human monoclonal antibody that binds to RANKL with high affinity and inhibits osteoclast differentiation and activation. Denosumab is administrated via subcutaneous injections in either the thigh, the abdomen or the back of the arm. From the site of injection, the drug is absorbed in the blood serum over time and reaches the surfaces of metabolising bone through the blood circulation. The serum drug concentration over time for denosumab has been modelled using the one-compartment PK model illustrated in Fig. 14 (see also Sect. 5.1) which takes into account the extra-vascular administration of the drug and the consequent absorption process from the injection site to the blood serum [97]. The blood serum represent the central compartment of the PK model, characterised by concentration, volume of distribution and bioavailability of the drug (i.e.,  $m_{den,ser}$  and  $V_d/F$ ). The process of drug absorption is described as a first order rate process characterised by the absorption rate  $k_{abs}$ . The drug was assumed to be cleared from the central compartment by both organs and enzymes. The elimination by organs was accounted for via the degradation rate  $k_{org}$ , whereas the elimination by enzymes was included via the degradation rate  $k_{enz}$  [146].

The degradation of the drug is assumed to be proportional to its concentration in the central compartment, however experimental data [90] suggested that the elimination process becomes limited above a certain threshold concentration ( $m_{den,ser}^{crit}$ ). According to enzyme kinetics [106], this limitation of the degradation has to be attributed to a limited capacity of the enzymes involved in the elimination process. The governing equations for the serum concentration of denosumab used in the PK model are the following:

**Fig. 14** Denosumab PK model: one-compartment PK model with central compartment characterized by concentration ( $m_{den,ser}$ ), volume of distribution and bioavailability of the drug ( $V_d/F$ ). Absorption process described via the absorption rate constant  $k_{abs}$ . Elimination process described via the two elimination constants  $k_{org}$  and  $k_{enz}$



$$\frac{dm_{den,ser}}{dt} = \begin{cases} k_{abs} \cdot m_{den,sub} - (k_{org} + k_{enz}) \cdot m_{den,ser} & \text{if } m_{den,ser} \leq m_{den,ser}^{crit} \\ k_{abs} \cdot m_{den,sub} - k_{org} \cdot m_{den,ser} - k_{enz} \cdot m_{den,ser}^{crit} & \text{if } m_{den,ser} \geq m_{den,ser}^{crit} \end{cases} \quad (19)$$

where  $m_{den,sub}$  is the amount of drug injected. From the start of the absorption process until when  $m_{den,ser}^{crit}$  is reached, the system is described via the first equation in Eq. (19). After this time the system follows the second equation. When the peak concentration is reached,  $m_{den,ser}$  starts to decrease reaching again  $m_{den,ser}^{crit}$ . From this point onwards the system follows the first equation.

To determine the parameters  $k_{abs}$ ,  $k_{org}$  and  $k_{enz}$ , clinical data measuring the temporal evolutions of denosumab serum concentration have been used [10]. Among the six different administration doses investigated in the clinical study, three have been used for the calibration of the model. Since denosumab is generally administered with a small number of high-doses injections, only the higher doses (ranging between 0.3 and 3 mg/kg) have been taken into account, assumed to be practically more relevant. Moreover, since the experimental data showed a limitation on denosumab degradation above a serum concentration of 750 ng/ml, this value has been assumed as threshold concentration  $m_{den,ser}^{crit}$  in the PK model. Since denosumab doses are administered according to the patient body mass, to compute the drug concentration in the model knowing the administered dose, an average subject of 70 kg body weight and a 3 litres volume of distribution central compartment (i.e.,  $F = 1$  and  $V_d/F = 3$  l) have been taken into account. The comparison between clinical data and the results obtained using the PK model for three different doses are illustrated in Fig. 15, where the markers indicate the experimental data and the curves the computed values. In particular, triangles, dots and circles represent measurements of denosumab concentration in patients for an administered dose of 0.3, 1 and 3 mg/kg respectively, and dotted, solid and dashed curves are the corresponding concentrations computed with the drug PK model. The continuous horizontal line indicates the threshold concentration.

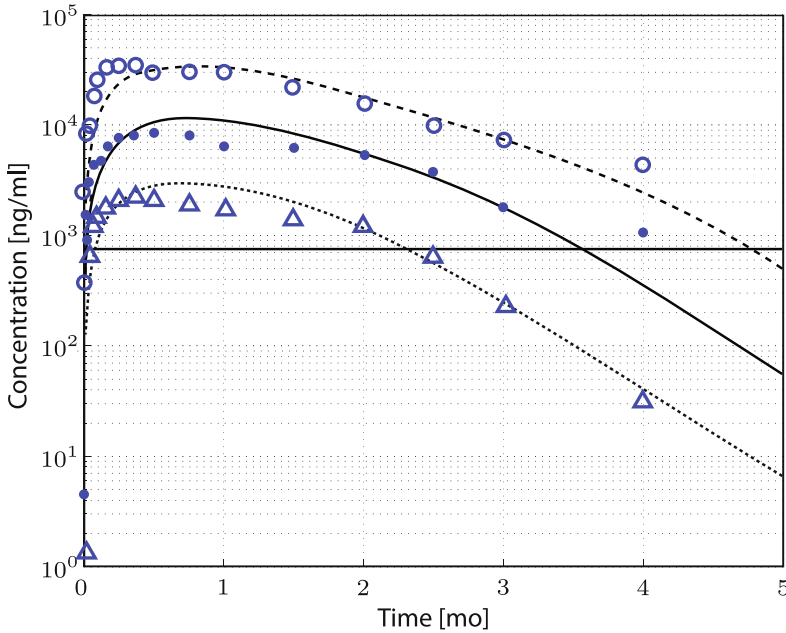


**Fig. 15** Calibration of the denosumab PK model: comparison between experimental (markers) and model-computed (curves) serum concentrations of denosumab over time. *Triangles* and *dotted curve* correspond to a drug dose of 0.3 mg/kg, *dots* and *solid curve* correspond to a dose of 1 mg/kg, *circles* and *dashed curve* correspond to a dose of 3 mg/kg. Solid horizontal line indicates  $m_{den,ser}^{crit}$

## 6.2 Mechanistic PK/PD Model of Osteoporosis

The biochemical interactions between bone cells and regulatory factors acting in the remodelling process were summarised in Sect. 2.2. Bone cell responses such as differentiation, proliferation and apoptosis are initiated via ligand-receptor binding reactions occurring on a particular cell. These reactions are based on the physical chemistry principles of mass balance and mass action kinetics applied to the receptor and its corresponding ligand [79]. Detailed development of the equations describing the law of mass action in the remodelling process can be found in the book chapter on bone cell interactions by Pivonka and co-workers [123].

The first mechanism-based model of bone remodelling was proposed by Lemaire and co-authors [88] and successively refined by Pivonka and co-workers [121, 122]. Since both those models took into account the major bone cell types involved in the remodelling process, together with the most significant regulatory factors, they are also referred to as *bone cell population models*. It is worth to mention that the model by Pivonka et al. also accounted for the changes in bone volume, providing in this way the pathway for a biomechanical extensions of the model. Previous models of bone remodelling and adaptation were mainly driven by mechanical loading. In this

context, a major advantage of the mechanism-based models is to provide a translation towards bone biology and clinical bone research. However, both the model from Lemaire et al. and the model from Pivonka et al. had the limitation of not including the concept of Frost's *mechanostat* [53], i.e., they lacked the inclusion of a biomechanical feedback. According to the mechanostat mechanism of action, bone overloading leads to increased bone formation responses, whereas bone underloading leads to increased bone resorption responses. This feedback warrants that, after sufficient time, bone reaches an equilibrium. Given the importance of a biomechanical feedback in the remodelling process, as a further development of the mechanism-based model, Pivonka and co-workers combined the bone cell population model with a micromechanical model of bone stiffness including the mechanostat concept [145]. The biomechanical feedback was included via the strain energy density (SED) induced in the bone matrix by the mechanical loading applied on bone at the macroscopic level. In particular, the loading at the macroscopic level has been linked to the loading at the microscopic level inducing microscopic deformations represented in the model by the SED, the latter parameter in turn affected the bone formation and resorption events by entering the bone cell population model. This mechanism-based model of bone remodelling has been used in combination with the denosumab PK model described in Sect. 6.1 to simulate PMO progression with and without drug intervention.

Due to the complexity of the bone remodelling process, it is not feasible to include into a mathematical model all the cell types and the regulatory factors involved. Therefore, the aim of a comprehensive model is to include sufficient details to address the scientific problem at hand. The mechanobiologically driven evolution of osteoblasts and osteoclasts were mathematically modelled by means of the bone cell population model, which explicitly considered several developmental stages of these cells. In particular, with reference to Fig. 16, the bone cell populations included in the model were: uncommitted osteoblast progenitors (OBu), osteoblast precursors (OBp), active osteoblasts (OBa), osteoclast precursors (OCp) and active osteoclasts (OCa). The progression of osteoblasts and osteoclasts along various developmental stages (i.e.,  $OBu \rightarrow OBp \rightarrow OBa$  and  $OCp \rightarrow OCa$ ) was implemented considering several regulatory mechanism (dashed arrows) which either activate (+) or repress (−) a certain cell function. Among these regulatory factors, there were the RANK-RANKL-OPG pathway regulating the differentiation of osteoclasts via the osteoblast lineage, and the effect of TGF- $\beta$  on OBu, OBp and OCa. Moreover, osteocytes were assumed to sense the SED ( $\Psi_{bm}$ ) induced in the bone matrix by the mechanical loading ( $\sigma$ ) and accordingly send a signal to OBp to promote either their proliferation (i.e., anabolic response) or the RANKL production (i.e., catabolic response). In addition, the action of denosumab and the progression of PMO were also included in the model as regulatory mechanisms. The former was accounted for via competitive binding reactions in the RANK-RANKL-OPG pathway, while the latter was included via disease-related RANKL increased production and mechanoresponsiveness reduction. Note that in Fig. 16 the fine dashed lines indicate binding reactions (i.e., RANK-RANKL-OPG plus denosumab and PTH binding to its recep-

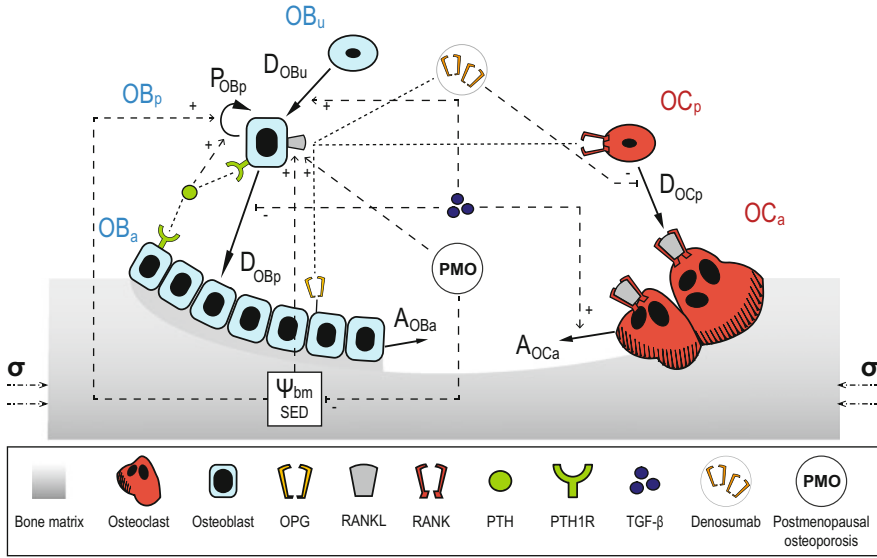


**Fig. 16** Mechanism-based model of bone remodelling showing: (i) osteoblast lineage comprising marrow stromal cells (uncommitted osteoblasts, OBU), osteoblast precursors (OBp), active osteoblasts (OBa); (ii) osteoclast lineage comprising osteoclast precursors (OCp) and active osteoclasts (OCa); (iii) RANK-RANKL-OPG pathway; (iv) TGF- $\beta$  action; (v) PTH action; (vi) denosumab competitive binding in the RANK-RANKL-OPG pathway; (vii) PMO effect; (viii) tissue scale loading ( $\sigma$ ) inducing the SED ( $\psi_{bm}$ ) in the bone matrix [121, 122, 145]

tor), the dashed arrows represent regulatory mechanisms and the solid arrows indicate either cells differentiation, proliferation or apoptosis.

The governing equations of the bone cell population model have been formulated as cell balance equations describing in and out flows of cells from the respective cell pools. Three ordinary differential equations (ODEs) were used to describe the changes in osteoblast precursor, active osteoblast and active osteoclast pool concentrations respectively. In addition, an ODE was used to describe the change in the bone matrix volume fraction ( $f_{bm}$ ) computed as the difference between the amount of bone resorbed and formed. The 4 ODEs constituting the system of equation governing the bone remodelling process are as follows:

$$\begin{aligned}
 \frac{dOBp}{dt} &= D_{OBu} \cdot OBU \cdot \pi_{act, OBU}^{TGF\beta} + P_{OBp} \cdot OBp \cdot \Pi_{act, OBp}^{mech} - D_{OBp} \cdot OBp \cdot \pi_{rep, OBp}^{TGF\beta}, \\
 \frac{dOBa}{dt} &= D_{OBp} \cdot OBp \cdot \pi_{rep, OBp}^{TGF\beta} - A_{OBa} \cdot OBa, \\
 \frac{dOCa}{dt} &= D_{OCp} \cdot OCp \cdot \pi_{act, OCp}^{RANKL} - A_{OCa} \cdot OCa \cdot \pi_{act, OCa}^{TGF\beta}, \\
 \frac{df_{bm}}{dt} &= -K_{res} \cdot OCa + K_{form} \cdot OBa,
 \end{aligned} \tag{20}$$

where  $D_{OBu}$ ,  $D_{OBp}$  and  $D_{OCp}$  are differentiation rates of uncommitted osteoblast progenitors, osteoblast precursors and osteoclast precursors respectively.  $P_{OBp}$  denotes the proliferation rate of osteoblast precursors.  $A_{OBa}$  and  $A_{OCa}$  are respectively the apoptosis rates of active osteoblasts and osteoclasts.  $K_{res}$  and  $K_{form}$  are respectively the bone resorption and bone formation rates. All the  $\pi$  together with  $\Pi$  represent regulatory functions.

At the core of any mechanism-based model of bone pathophysiology is how various regulatory factors govern the cell behaviour. When dealing with extracellular ligands that bind to their specific receptors on a cell surface (e.g., systemic hormones, autocrine and paracrine factors, growth factors) the behaviour of the cell is modulated by the activation of specific intracellular signalling pathways initiated by the receptor-ligand binding. These intracellular pathways induce an overall cell response that can be either cell differentiation, proliferation and apoptosis or the expression of signalling molecules and receptors. The formulation of binding reactions based on the law of mass action kinetics allows the derivation of phenomenological Hill-type functions that can either activate or repress a particular cell behaviour [86]. In the bone cell population model described so far, these regulatory functions were introduced both as *activator* ( $\pi_{act}$ ) and *repressor* ( $\pi_{rep}$ ) functions, i.e. functions that can either promote or inhibit differentiation, proliferation and apoptosis of the cells. In particular, TGF- $\beta$  binding to its receptors has been accounted for via  $\pi_{act,OBu}^{TGF\beta}$ ,  $\pi_{rep,OBp}^{TGF\beta}$  and  $\pi_{act,OCa}^{TGF\beta}$ ; the competitive binding between RANK, RANKL, OPG and denosumab has been included via  $\pi_{act,OCp}^{RANKL}$ ,  $\Psi_{bm}$  regulating the proliferation of OBp has been introduced via  $\Pi_{act,OBp}^{mech}$ . For a complete description and derivation of the governing equations refer to [146].

### 6.3 Modelling Disease Progression in PMO

Experimental studies investigating the pathophysiology of PMO indicated that the disease progression could depend on several regulatory mechanisms perturbed at the same time. Among the potential pathogenic mechanisms driving PMO, oestrogen deficiency has been widely accepted as the principal cause of PMO [96, 133] resulting in increased osteoclast and osteoblast concentrations and consequently increased bone turnover compared to the normal remodelling homeostasis [54]. Furthermore, it appears that another effect of oestrogen deficiency is a decrease in bone mechanoresponsiveness due to increased osteocyte apoptosis. In the initial phase of the oestrogen deficiency, the increase in osteoclast concentration is higher than the increase in osteoblast concentration, inducing a significant bone loss right after the onset of PMO (we also refer to this as first phase of PMO). Simultaneously, the first phase of PMO is also characterised by an increased RANKL/OPG ratio. After a period of time that can vary between some months and few years, the rate of bone loss decreases and bone is subjected to a long-lasting moderate bone loss thereafter (second phase of PMO).

In the mechanism-based model of bone remodelling described in Sect. 6.2 PMO has been modelled introducing a disease-related increase in the RANKL production, which led to an increased osteoclast differentiation. In order to account for the moderate bone loss characterising the second phase of PMO, the excessive production of RANKL has been assumed to reduce over time. The reduction in bone mechanoresponsiveness has also been introduced in the model by varying the parameters governing the sensitivity of bone remodelling to a changing mechanical load [146].

## 6.4 Modelling the Action of Denosumab

Denosumab acts similarly to OPG and competes with RANK and OPG in the binding with RANKL. Specifically, the higher the denosumab concentration, the lower the concentration of RANKL-RANK complexes. In the mechanism-based model of bone remodelling described in Sect. 6.2 denosumab has been introduced as co-regulator factor of osteoclast differentiation by means of the activator function  $\pi_{act, OCP}^{RANKL}$ . Precisely, the simulation of denosumab treatment induced a reduction of the RANKL-RANK complexes concentration, which consequently downregulated the activator function and eventually resulted in a lower fraction of osteoclast precursor cells differentiated into active osteoclasts. This reduction in the active osteoclast number induced a decreased bone resorption. Adapting the approach used by Pivonka and co-authors [121], the concentration of RANKL was expressed via Eq. (21) taking into account the action of denosumab in the competitive binding:

$$RANKL = RANKL^{max} \cdot \frac{\beta_{RANKL} + P_{RANKL}}{\beta_{RANKL} + \tilde{D}_{RANKL} \cdot RANKL^{max}} \cdot (1 + K_{a, RANKL-OPG} \cdot OPG + K_{a, RANKL-RANK} \cdot RANK + \zeta \cdot K_{a, RANKL-d} \cdot den)^{-1}, \quad (21)$$

where  $K_{a, RANKL-OPG}$ ,  $K_{a, RANKL-RANK}$  and  $K_{a, RANKL-d}$  are the equilibrium association binding constants respectively for the binding of RANKL to OPG, RANKL to RANK and RANKL to denosumab.  $OPG$ ,  $RANK$  and  $den$  represent the molar concentrations of OPG, RANK, and denosumab respectively.  $\beta_{RANKL}$  is the intrinsic RANKL production rate,  $P_{RANKL}$  is the external RANKL dosage term,  $\tilde{D}_{RANKL}$  is the constant degradation rate.  $RANKL^{max}$  is the maximum concentration of RANKL [146]. It is worth to notice that the concentrations of regulatory factors in the model (i.e., RANKL, OPG, RANK and TGF- $\beta$ ) have been formulated for a specific representative volume element (RVE) of bone tissue, while the concentration of denosumab was expressed in blood serum using the PK model described in Sect. 6.1. To be able to express the concentration of denosumab in the bone RVE, an additional compartment has been taken into account in the model, i.e., the bone RVE compartment. Assuming an instantaneous distribution from the serum compartment

into the bone RVE compartment, the concentration in the bone RVE compartment was considered to be equal to the serum concentration. To include the possibility of limited accessibility of the drug in the bone RVE compartment, the accessibility factor  $\zeta$  has been introduced in Eq. (21). In particular,  $\zeta = 1$  was assumed to indicate unrestricted access to denosumab and  $\zeta < 1$  reflected access restrictions. Knowing the RANKL concentration from Eq. (21), the concentration of the RANKL-RANK complexes was expressed as follows:

$$[RANKL - RANK] = K_{a,RANKL-RANK} \cdot RANKL \cdot RANK. \quad (22)$$

Consequently, the activator function was defined as:

$$\pi_{act,OCp}^{RANKL} = \frac{[RANK - RANKL]}{K_{d,RANKL-d} + [RANKL - RANK]}, \quad (23)$$

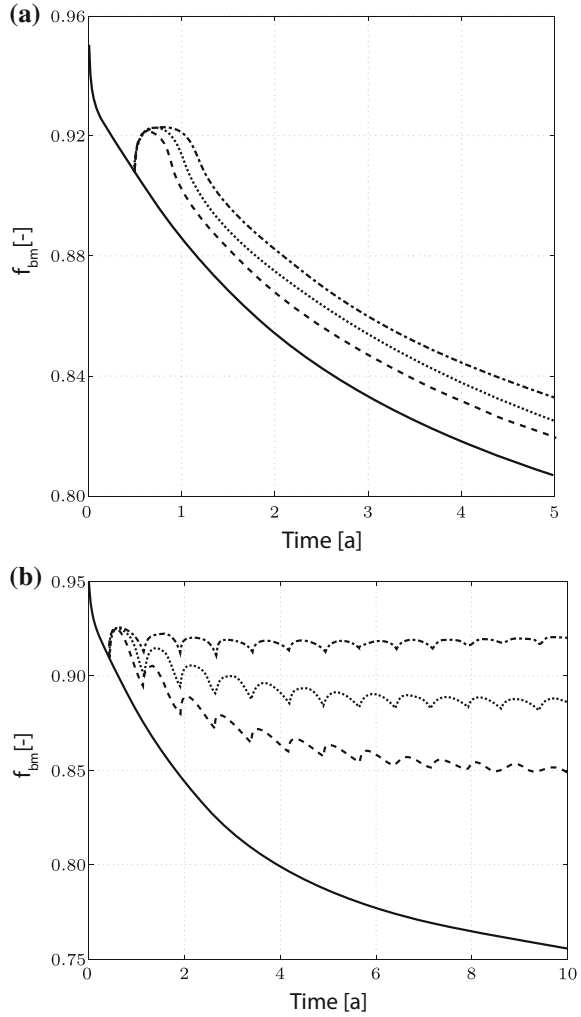
where  $K_{d,RANKL-d}$  indicates the corresponding equilibrium dissociation binding constant.

## 6.5 Numerical Simulations

The results of the numerical simulations of PMO progression and denosumab treatments are illustrated in Fig. 17 showing the change of  $f_{bm}$  over time. The solid curves represent the disease progression of PMO over 5 (Fig. 17a) and 10 years (Fig. 17b) respectively. It is clearly visible that the bone loss obtained in the simulations is rapid in the first 5 years, while it slows down thereafter. In addition, it is worth to notice that the shape of the PMO progression curve obtained with the mechanism-based model of bone remodelling appears similar to the shape of the asymptotic disease progression reported in Fig. 12. However, while in Fig. 12 the shape of the curve was decided a priori by choosing an asymptotic disease progression model, in Fig. 17 the shape of the curve resulted from the structure of the mechanism-based bone remodelling model and the way in which the biochemical and biomechanical feedback and PMO were modelled.

The results of the simulations of PMO treatments with single and multiple injections of denosumab are reproduced in Fig. 17a, b respectively. The three non-solid curves represent simulations with three different drug doses, specifically: the dashed curves correspond to 0.3 mg/kg, the dot curves correspond to 1.0 mg/kg and the dash-dot curves correspond to 3.0 mg/kg. The results for the single injection indicate that the bone loss was rapidly reduced after the injection of the drug. In addition, even though the increase in the  $f_{bm}$  appeared to be independent of the dose level, the higher the dose of denosumab the longer the effect on  $f_{bm}$  (i.e., time in which  $f_{bm}$  stays constant at a certain level). Overall, the observed bone gain was small and once denosumab was cleared, the bone loss continued along the trajectory of PMO. Therefore, the action of a treatment with a single injection of denosumab can be assumed as

**Fig. 17** Changes of cortical  $f_{bm}$  over time for PMO and different denosumab administration regimes: **a** single injection, **b** multiple injections. *Solid curves* indicate PMO progression without drug treatment, *dashed curves* indicate treatment with a denosumab dose of 0.3 mg/kg, *dotted curves* indicates treatment with a denosumab dose of 1.0 mg/kg, *dash-dot curves* indicate treatment with a denosumab dose of 3.0 mg/kg



symptomatic because it does not affect the disease progression. In the investigation of multiple injections of denosumab, the drug administration has been modelled as one injection every 9 months. The reduced bone loss appeared to be dependent on the dose level with a lower anti-catabolic effect corresponding to lower doses. The highest dose significantly reduced the bone loss maintaining the  $f_{bm}$  at a higher and almost constant level.

## 7 Summary and Conclusions

This chapter reviewed the complexity of the pathophysiology of the skeletal system and the numerous regulatory factors involved at multiple scales in bone homeostasis and OP. Current approaches taken to understand this system include clinical research, basic bone biology and biomechanical assessment. It is evident that none of these approaches alone will be able to provide a comprehensive picture of the skeletal system and that a combination of all the information gained separately is required. In this context, DSA is a promising framework which allows to link together various disciplines and to utilise information on bone pathophysiology based on the major bone biomarkers in a quantitative way. It also provides the ability to define clearer clinical endpoints and better assess drug efficacy. If based on subject-specific data, the DSA approach gives the possibility to formulate subject-specific models allowing the optimisation of individual treatments rather than drawing conclusions on a population basis.

The use of comprehensive mechanism-based models of bone remodelling in DSA allows quantitative assessment of treatment efficacy at various levels of bone pathophysiology. To continuously improve these models good experimental data and up-to-date computational modelling tools are crucial. As with any mathematical approach, the identification from available experimental data of the essential time and rate limiting steps in the bone remodelling process is necessary. Moreover, in order for those models to be relevant for clinical and basic bone biology research, the most important aspects of bone physiology need to be incorporated.

In conclusion, the ultimate goal of DSA is to develop a quantitative simulation tool which allows the prediction of short-term and long-term effects of various drug treatments (including combinations of drugs) on disease progression in OP and other bone diseases. As such, the computational model needs to undergo continuous development according to the latest discoveries in the bone remodelling process and associated biomarkers, in order to increase its ability to compare, predict and extrapolate drug treatment effects. Currently, the development of fully mechanistic disease system models for OP is an ongoing process, it is anticipated that in the near future these models will be able to adequately predict the long-term effects of drug treatment on the clinical outcome, i.e., bone fractures.

### Outlook to Future Model Extensions

One possible model extension is towards a whole organ scale description of calcium and phosphate homeostasis. Key regulatory factors in the endocrine control of calcium concentration are PTH and vitamin D. Bone plays an important part in the calcium and phosphate homeostasis, other organs involved include gut (responsible of mineral absorption) and kidneys (responsible for calcitriol formation). Many endocrine diseases such as hyperparathyroidism and hypoparathyroidism have a high impact on the bone remodelling balance and consequently on bone health. The loss of kidney functions has a significant impact on bone health as well. In this context, Peterson and Riggs have developed a physiologically based mathematical model of

integrated calcium homeostasis and bone remodelling containing 46 ODEs which describe the concentration of calcium and phosphate in the different body compartments such as blood, gut [119].

Another important model extension is towards *spatio-temporal* disease progression models. As previously discussed, bone fractures result from the combination of the applied mechanical load and the material properties of bone (including porosity and TMD). Bone fractures are localised phenomena which initiate at a particular spatial location within bone. In order to predict bone fracture and the evolving failure pattern more accurately, spatio-temporal mechanical models of bone are required. Researchers in the field of materials engineering developed a large variety of constitutive models of bone which are able to simulate bone fracture under known mechanical loading conditions. However, these models did not integrate the bone remodelling process in their framework, but were purely mechanical. A first attempt to develop spatio-temporal models of bone disease progression were made by Pivonka and co-workers who studied the age-related expansion of the marrow cavity and the trabecularisation of cortical bone using a mechanobiological model [89].

**Acknowledgements** Dr Pivonka acknowledges support of this work by the Australian Research Council (ARC). Miss Trichilo acknowledges support by The University of Melbourne as part of the International PhD scholarship program.

## References

1. E. Abe, M. Yamamoto, Y. Taguchi, B. Lecka-Czernik, C.A. O'Brien, A.N. Economides, N. Stahl, R.L. Jilka, S.C. Manolagas, Essential requirement of BMPs-2/4 for both osteoblast and osteoclast formation in murine bone marrow cultures from adult mice: Antagonism by noggin. *J. Bone Mineral Res.* **15**(4), 663–673 (2000)
2. M.E. Arlot, E. Sornay-Rendu, P. Garnero, B. Vey-Marty, P.D. Delmas, Apparent pre- and postmenopausal bone loss evaluated by DXA at different skeletal sites in women: the OFELY cohort. *J. Bone Mineral Res.* **12**(4), 683–690 (1997)
3. Y. Bala, D. Farlay, P.D. Delmas, P.J. Meunier, G. Boivin, Time sequence of secondary mineralization and microhardness in cortical and cancellous bone from ewes. *Bone* **46**(4), 1204–1212 (2010). ISSN 8756-3282
4. Y. Bala, D. Farlay, G. Boivin, Bone mineralization: from tissue to crystal in normal and pathological contexts. *Osteoporosis Int.* **24**(8), 2153–2166 (2013). ISSN 1433-2965
5. Y. Bala, R. Zebaze, E. Seeman, Role of cortical bone in bone fragility. *Current Opinion Rheumatol.* **27**(4), 406–413 (2015)
6. R. Baron, E. Hesse, Update on bone anabolics in osteoporosis treatment: rationale, current status, and perspectives. *J. Clin. Endocrinol. Metaboli.* **97**(2), 311–325 (2012). ISSN 0021972X
7. R. Baron, M. Kneissel, WNT signaling in bone homeostasis and disease: from human mutations to treatments. *Nat. Med.* **19**(2), 179–92 (2013). ISSN 1546-170X
8. C.A. Baud, M. Gossi, Degree of mineralization of bone tissue as determined by quantitative microradiography: effect of age, sex and pathological conditions, in *Proceedings Fourth International Conference on Bone Measurement* (1980)
9. D.C. Bauer, A. Schwartz, L. Palermo, J. Cauley, M. Hochberg, A. Santora, S.R. Cummings, D.M. Black, Fracture prediction after discontinuation of 4 to 5 years of alendronate therapy. *JAMA Int. Med.* **174**(7), 1126–34 (2014). ISSN 2168-6106

10. P.J. Bekker, D.L. Holloway, A.S. Rasmussen, R. Murphy, S.W. Martin, P.T. Leese, G.B. Holmes, C.R. Dunstan, A.M. DePaoli, A single-dose placebo-controlled study of AMG 162, a fully human monoclonal antibody to RANKL, in postmenopausal women. *J. Bone Mineral Res.* **19**(7), 1059–1066 (2004). ISSN 0884-0431
11. C. Bergot, Y. Wu, E. Jolivet, L.Q. Zhou, J.D. Laredo, V. Bousson, The degree and distribution of cortical bone mineralization in the human femoral shaft change with age and sex in a microradiographic study. *Bone* **45**(3), 435–442 (2009)
12. J.P. Bilezikian, Combination anabolic and antiresorptive therapy for osteoporosis: opening the anabolic window. *Current Osteoporosis Rep.* **6**(1), 24–30 (2008). ISSN 1544-2241
13. D.M. Black, C.J. Rosen, Postmenopausal osteoporosis. *N. Engl. J. Med.* **374**(3), 254–262 (2016)
14. J.M. Bland, D.G. Altman, Statistical methods for assessing agreement between two methods of clinical measurement. *Lancet* **1**(8476), 307–310 (1986). ISSN 01406736
15. R.D. Blank, D.G. Malone, R.C. Christian, N.L. Vallarta-Ast, D.C. Krueger, M.K. Drezner, N.C. Binkley, K.E. Hansen, Patient variables impact lumbar spine dual energy X-ray absorptiometry precision. *Osteoporosis Int.* **17**(5), 768–774 (2006). ISSN 1433-2965
16. G. Boivin, P. Meunier, Effects of bisphosphonates on matrix mineralization. *J. Musculoskelet. Neuronal Interact.* **2**(6), 538–543 (2002)
17. G. Boivin, P.J. Meunier, The degree of mineralization of bone tissue measured by computerized quantitative contact microradiography. *Calcif. Tissue Int.* **70**(6), 503–511 (2002)
18. G. Boivin, D. Farlay, Y. Bala, A. Doublier, P.J. Meunier, P.D. Delmas, Influence of remodeling on the mineralization of bone tissue. *Osteoporosis Int.* **20**(6), 1023–1026 (2009). ISSN 1433-2965
19. G.Y. Boivin, P.M. Chavassieux, A.C. Santora, J. Yates, P.J. Meunier, Alendronate increases bone strength by increasing the mean degree of mineralization of bone tissue in osteoporotic women. *Bone* **27**(5), 687–694 (2000)
20. J. Borggreffe, C. Graeff, T.N. Nickelsen, F. Marin, C.C. Gler, Quantitative computed tomographic assessment of the effects of 24 months of teriparatide treatment on 3D femoral neck bone distribution, geometry, and bone strength: results from the EUROFOR study. *J. Bone Mineral Res.* **25**(3), 472–481 (2010). ISSN 1523-4681
21. M.L. Bouxsein, Mechanisms of osteoporosis therapy: a bone strength perspective. *Clin. Cornerstone* **5**, S13–S21 (2003). ISSN 1098-3597
22. W.J. Boyle, W.S. Simonet, D.L. Lacey, Osteoclast differentiation and activation. *Clin. Calcium* **17**(4), 484–492 (2003). ISSN 0028-0836
23. J. Burch, St. Rice, H. Yang, A. Neilson, L. Stirk, R. Francis, P. Holloway, S. Peter, D. Craig, Systematic review of the use of bone turnover markers for monitoring the response to osteoporosis treatment: the secondary prevention of fractures, and primary prevention of fractures in high-risk groups. Report ISSN1366-5278, National Institute for Health Research (2014)
24. A.J. Burghardt, G.J. Kazakia, S. Ramachandran, T.M. Link, S. Majumdar, Age and gender related differences in the geometric properties and biomechanical significance of intra-cortical porosity in the distal radius and tibia. *J. Bone Mineral Res.* **25**(5), 983–993 (2010). ISSN 0884-0431
25. D.B. Burr, Bone quality: understanding what matters. *J. Musculoskelet. Neuronal Interact.* **4**(2), 184–186 (2004). ISSN 11087161
26. L.M. Calvi, G.B. Adams, K.W. Weibrecht, J.M. Weber, D.P. Olson, M.C. Knight, R.P. Martin, E. Schipani, P. Divieti, F.R. Bringhurst, L.A. Milner, H.M. Kronenberg, D.T. Scadden, Osteoblastic cells regulate the haematopoietic stem cell niche. *Nature* **425**(6960), 841–846 (2003)
27. D.R. Carter, W.C. Hayes, Bone compressive strength: the influence of density and strain rate. *Science* **194**(4270), 1174–1176 (1976)
28. T.J. Chambers, Osteoblasts release osteoclasts from calcitonin-induced quiescence. *J. Cell Sci.* **57**, 247–260 (1982)
29. P.L.S. Chan, N.H.G. Holford, Drug treatment effects on disease progression. *Annu. Rev. Pharmacol. Toxicol.* **41**(1), 625–659 (2001)

30. L. Cianferotti, F. DAsta, M.L. Brandi, A review on strontium ranelate long-term antifracture efficacy in the treatment of postmenopausal osteoporosis. *Therapeutic Adv. Musculoskeletal Disease* **5**(3), 127–139 (2013). ISSN 1759-720X
31. T.L. Clemens, G. Karsenty, The osteoblast: an insulin target cell controlling glucose homeostasis. *J. Bone Mineral Res.* **26**(4), 677–680 (2011)
32. P. Close, A. Neuprez, J.-Y. Reginster, Developments in the pharmacotherapeutic management of osteoporosis. *Expert Opinion Pharmacother.* **7**(12), 1603–1615 (2006). ISSN 1465-6566
33. D.M.L. Cooper, B. Erickson, A.G. Peele, K. Hannah, C.D.L. Thomas, J.G. Clement, Visualization of 3D osteon morphology by synchrotron radiation micro-CT. *J. Anatomy* **219**(4), 481–489 (2011). ISSN 0021-8782
34. F. Cosman, Anabolic and antiresorptive therapy for osteoporosis: combination and sequential approaches. *Current Osteoporosis Rep.* **12**(4), 385–395 (2014). ISSN 1544-2241
35. F. Cosman, R.A. Wermers, C. Recknor, K.F. Mauck, L. Xie, E.V. Glass, J.H. Kregge, Effects of teriparatide in postmenopausal women with osteoporosis on prior alendronate or raloxifene: differences between stopping and continuing the antiresorptive agent. *J. Clin. Endocrinol. Metab.* **94**(10), 3772–3780 (2009). ISSN 0021-972X
36. S. Cremers, P. Garnero, Biochemical markers of bone turnover in the clinical development metastatic bone disease potential uses and pitfalls. *Drugs* **66**(16), 2031–2058 (2006)
37. S.R. Cummings, D. Bates, D.M. Black, Clinical use of bone densitometry: scientific review. *JAMA* **288**(15), 1889–1897 (2002)
38. J.D. Currey, The mechanical properties of bone. *Clin. Orthop. Relat. Res.* **73**, 210–231 (2006)
39. J.D. Currey, K. Brear, P. Zioupos, The effects of ageing and changes in mineral content in degrading the toughness of human femora. *J. Biomech.* **29**(2), 257–260 (1996)
40. M. Danhof, G. Alvan, S.G. Dahl, J. Kuhlmann, G. Paintaud, Mechanism-based pharmacokinetic-pharmacodynamic modeling – a new classification of biomarkers. *Pharm. Res.* **22**(9), 1432–1437 (2005). ISSN 0724-8741
41. M. Danhof, J. de Jongh, E.C.M. De Lange, O. Della Pasqua, B.A. Ploeger, R.A. Voskuyl, Mechanism-based pharmacokinetic-pharmacodynamic modeling: biophase distribution, receptor theory, and dynamical systems analysis. *Annu. Rev. Pharmacol. Toxicol.* **47**, 357–400 (2007). ISSN 0362-1642
42. D.W. Dempster, M.W. Ferguson-Pell, R.W. Mellish, G.V. Cochran, F. Xie, C. Fey, W. Horbert, M. Parisien, R. Lindsay, Relationships between bone structure in the iliac crest and bone structure and strength in the lumbar spine. *Osteoporos. Int.* **3**(2), 90–96 (1993)
43. A. El Maghraoui, L. Achemlal, A. Bezza, Monitoring of dual-energy X-ray absorptiometry measurement in clinical practice. *J. Clin. Densitom.* **9**(3), 281–286 (2006). ISSN 1094-6950
44. E.F. Eriksen, Cellular mechanisms of bone remodeling. *Rev. Endocr. Metab. Disord.* **11**(4), 219–227 (2010). ISSN 13899155
45. S. Ferrari, Future directions for new medical entities in osteoporosis. *Best Pract. Res. Clin. Endocrinol. Metab.* **28**(6), 859–870 (2014). ISSN 15321908
46. J.S. Finkelstein, J.J. Wyland, H. Lee, R.M. Neer, Effects of teriparatide, alendronate, or both in women with postmenopausal osteoporosis. *J. Clin. Endocrinol. Metab.* **95**(4), 1838–1845 (2010). ISSN 0021-972X
47. H. Follet, G. Boivin, C. Rumelhart, P.J. Meunier, The degree of mineralization is a determinant of bone strength: a study on human calcanei. *Bone* **34**(5), 783–789 (2004)
48. H. Follet, S. Viguet-Carrin, B. Burt-Pichat, B. Depalle, Y. Bala, E. Gineys, F. Munoz, M.E. Arlot, G. Boivin, R. Chapurlat, P.D. Delmas, M.L. Bouxsein, Effects of pre-existing micro-damage, collagen cross-links, degree of mineralization, age and architecture on compressive mechanical properties of elderly human vertebral trabecular bone. *J. Orthop. Res.* **29**(4), 481–488 (2011)
49. N. Fratzl-Zelman, P. Roschger, B.M. Misof, S. Pfeffer, F.H. Glorieux, K. Klaushofer, F. Rauch, Normative data on mineralization density distribution in iliac bone biopsies of children, adolescents and young adults. *Bone* **44**(6), 1043–1048 (2009)
50. H.M. Frost, in *Bone Remodelling Dynamics*, ed. by C.R. Lam (Charles C. Thomas, Springfield, 1963)

51. H.M. Frost, Dynamics of bone remodeling, in *Bone Biodynamics*, ed. by H.M. Frost (Little, Brown & Co, 1964), pp. 315–333
52. H.M. Frost, The skeletal intermediary organization. *Metab. Bone Disease Relat. Res.* **4**(5), 281–290 (1983). ISSN 02218747
53. H.M. Frost, Bone mass and the mechanostat: a proposal. *Anat Record* **219**(1), 1–9 (1987)
54. P. Garnero, E. Sornay-Rendu, M.C. Chapuy, P.D. Delmas, Increased bone turnover in late postmenopausal women is a major determinant of osteoporosis. *J. Bone Mineral Res.* **11**(3), 337–349 (1996). ISSN 0884-0431
55. P. Geusens, New insights into treatment of osteoporosis in postmenopausal women. *RMD Open* **1**(Suppl 1), e000051 (2015). ISSN 2056-5933
56. P. Geusens, R. Chapurlat, G. Schett, A. Ghasem-Zadeh, E. Seeman, J. de Jong, J. van den Bergh, High-resolution in vivo imaging of bone and joints: a window to microarchitecture. *Nat. Rev. Rheumatol.* **10**(5), 304–313 (2014). ISSN 1759-4790
57. A. Grey, M. Bolland, B. Mihov, S. Wong, A. Horne, G. Gamble, I.R. Reid, Duration of antiresorptive effects of low-dose zoledronate in osteopenic postmenopausal women: a randomized, placebo-controlled trial. *J. Bone Mineral Res.* **29**(1), 166–172 (2014). ISSN 1523-4681
58. D.J. Hadjidakis, I.I. Androulakis, Bone remodeling. *Ann. N. Y. Acad. Sci.* **1092**, 385–396 (2006). ISSN 00778923
59. K.D. Harrison, D.M.L. Cooper, Modalities for visualization of cortical bone remodeling: the past, present, and future. *Front. Endocrinol.* **6**, 122 (2015). ISSN 1664-2392
60. Ch. Hellmich, F.-J. Ulm, L. Dormieux, Can the diverse elastic properties of trabecular and cortical bone be attributed to only a few tissue-independent phase properties and their interactions? *Biomech. Model. Mechanobiol.* **2**(4), 219–238 (2004). ISSN 1617-7940
61. K. Henriksen, D.J. Leeming, C. Christiansen, M.A. Karsdal, Use of bone turnover markers in clinical osteoporosis assessment in women: current issues and future options. *Women's Health* **7**(6), 689–698 (2011). ISSN 1745-5057
62. C.J. Hernandez, How can bone turnover modify bone strength independent of bone mass? *Bone* **42**(6), 1014–1020 (2008). ISSN 87563282
63. C.J. Hernandez, T.M. Keaveny, A biomechanical perspective on bone quality. *Bone* **39**(6), 1173–1181 (2006). ISSN 8756-3282
64. L.C. Hofbauer, M. Schoppet, Clinical implications of the osteoprotegerin/RANKL/RANK system for bone. *J. Am. Med. Assoc.* **292**(4), 490–495 (2004)
65. N.H.G. Holford, Clinical pharmacology = disease progression + drug action. *Br. J. Clin. Pharmacol.* **79**(1), 18–27 (2013). ISSN 1365-2125
66. N.H.G. Holford, L.B. Sheiner, Kinetics of pharmacologic response. *Pharmacol. Ther.* **16**(2), 143–166 (1982). ISSN 01637258
67. N.J. Horwood, J. Elliott, T.J. Martin, M.T. Gillespie, Osteotropic agents regulate the expression of osteoclast differentiation factor and osteoprotegerin in osteoblastic stromal cells. *Endocrinology* **139**(11), 4743 (1998)
68. S.L. Hui, C.W. Slemenda, C.C. Johnston, Age and bone mass as predictors of fracture in a prospective study. *J. Clin. Investig.* **81**(6), 1804–1809 (1988). ISSN 0021-9738
69. Z.F.G. Jaworski, C. Hooper, Study of cell kinetics within evolving secondary haversian systems. *J. Anat.* **131**(1), 91–102 (1980)
70. Z.F.G. Jaworski, B. Duck, G. Sekaly, Kinetics of osteoclasts and their nuclei in evolving secondary haversian systems. *J. Anat.* **133**, 397405 (1981)
71. W.S.S. Jee, W. Yao, Overview: animal models of osteopenia and osteoporosis. *J. Musculoskelet. Neuron Interact.* **1**(3), 193–207 (2001)
72. W.S.S. Jee, X.Y. Tian, R.B. Setterberg, Cancellous bone minimodeling-based formation: a Frost Takahashi legacy. *J. Musculoskelet. Neuronal Interact.* **7**(3), 232–239 (2007)
73. B. Jobke, B. Muehe, A.J. Burghardt, J. Semler, T.M. Link, S. Majumdar, Teriparatide in bisphosphonate-resistant osteoporosis: Microarchitectural changes and clinical results after 6 and 18 months. *Calcif. Tissue Int.* **89**(2), 130–139 (2011). ISSN 1432-0827
74. J.A. Kanis, Diagnosis of osteoporosis and assessment of fracture risk. *Lancet* **359**(9321), 1929–1936 (2002). ISSN 0140-6736

75. J.A. Kanis, N. Burlet, C. Cooper, P.D. Delmas, J.Y. Reginster, F. Borgstrom, R. Rizzoli, European guidance for the diagnosis and management of osteoporosis in postmenopausal women. *Osteoporos. Int.* **19**(4), 399–428 (2008). ISSN 0937941X
76. J.A. Kanis, E.V. McCloskey, H. Johansson, C. Cooper, R. Rizzoli, J.Y. Reginster, European guidance for the diagnosis and management of osteoporosis in postmenopausal women. *Osteoporos. Int.* **24**(1), 23–57 (2013). ISSN 1433-2965
77. Y. Kawano, R. Kypta, Secreted antagonists of the Wnt signalling pathway. *J. Cell Sci.* **116**(13), 2627–2634 (2003)
78. A.E. Kearns, S. Khosla, P.J. Kostenuik, Receptor activator of nuclear factor  $\kappa$ b ligand and osteoprotegerin regulation of bone remodeling in health and disease. *Endocr. Rev.* **29**(2), 155–192 (2008). ISSN 0163-769X
79. J. Keener, J. Sneyd, *Mathematical Physiology*, 2nd edn. (Springer, Berlin, 2009). ISBN 9780387758466
80. L.J. Kidd, A.S. Stephens, J.S. Kuliwaba, N.L. Fazzalari, A.C.K. Wu, M.R. Forwood, Temporal pattern of gene expression and histology of stress fracture healing. *Bone* **46**(2), 369–378 (2010)
81. R. Kulkarni, A. Bakker, V. Everts, J. Klein-Nulend, Inhibition of osteoclastogenesis by mechanically loaded osteocytes: Involvement of MEPE. *Calcif. Tissue Int.* **87**(5), 461–468 (2010)
82. D.L. Lacey, E. Timms, H.L. Tan, M.J. Kelley, C.R. Dunstan, T. Burgess, R. Elliott, A. Colombero, G. Elliott, S. Scully, H. Hsu, J. Sullivan, N. Hawkins, E. Davy, C. Caparelli, A. Eli, Y.X. Qian, S. Kaufman, I. Sarosi, V. Shalhoub, G. Senaldi, J. Guo, J. Delaney, W.J. Boyle, Osteoprotegerin ligand is a cytokine that regulates osteoclast differentiation and activation. *Cell* **93**, 165–176 (1998). ISSN 00928674
83. J. Lam, S. Takeshita, J.E. Barker, O. Kanagawa, F.P. Ross, S.L. Teitelbaum, TNF- $\alpha$  induces osteoclastogenesis by direct stimulation of macrophages exposed to permissive levels of RANK ligand. *J. Clin. Invest.* **106**(12), 1481–1488 (2000)
84. L.E. Lanyon, Osteocytes, strain detection, bone modeling and remodeling. *Calcif. Tissue Int.* **53**, S102–S107 (1993)
85. L.E. Lanyon, S. Bourn, The influence of mechanical function on the development and remodeling of the tibia. an experimental study in sheep. *J. Bone Joint Surg. Am.* **61**(2), 263–273 (1979)
86. D.A. Lauffenburger, J. Linderman, *Receptors: Models for Binding, Trafficking, and Signaling* (Oxford University Press, New York, 1993)
87. D.J. Leeming, P. Alexandersen, M.A. Karsdal, P. Qvist, S. Schaller, L.B. Tankó, An update on biomarkers of bone turnover and their utility in biomedical research and clinical practice. *Eur. J. Clin. Pharmacol.* **62**(10), 781–792 (2006). ISSN 00316970
88. V. Lemaire, F.L. Tobin, L.D. Greller, C.R. Cho, L.J. Suva, Modeling the interactions between osteoblast and osteoclast activities in bone remodeling. *J. Theor. Biol.* **229**(3), 293–309 (2004)
89. C. Lerebours, P.R. Buenzli, S. Scheiner, P. Pivonka, A multiscale mechanobiological model of bone remodelling predicts site-specific bone loss in the femur during osteoporosis and mechanical disuse. *Biomech. Model. Mechanobiol.* **15**(1), 43–67 (2015)
90. E.M. Lewiecki, Treatment of osteoporosis with denosumab. *Maturitas* **66**, 182–186 (2010). ISSN 03785122
91. T. Lin, C. Wang, X.Z. Cai, X. Zhao, M.M. Shi, Z.M. Ying, F.Z. Yuan, C. Guo, S.G. Yan, Comparison of clinical efficacy and safety between denosumab and alendronate in postmenopausal women with osteoporosis: a meta-analysis. *Int. J. Clin. Pract.* **66**(4), 399–408 (2012). ISSN 1742-1241
92. R. Lindsay, W.H. Scheele, R. Neer, et al, Sustained vertebral fracture risk reduction after withdrawal of teriparatide in postmenopausal women with osteoporosis. *Arch. Intern. Med.* **164**(18), 2024–2030 (2004). ISSN 0003-9926
93. X.S. Liu, L. Ardeshirpour, J.N. VanHouten, E. Shane, J.J. Wysolmerski, Site-specific changes in bone microarchitecture, mineralization, and stiffness during lactation and after weaning in mice. *J. Bone Mineral Res.* **27**(4), 865–875 (2012). ISSN 15234681

94. Y. Lu, H.K. Genant, J. Shepherd, S. Zhao, A. Mathur, T.P. Fuerst, S.R. Cummings, Classification of osteoporosis based on bone mineral densities. *J. Bone Mineral Res.* **16**(5), 901–910 (2001). ISSN 1523-4681
95. Z.F. Lu, G. Wang, C.R. Dunstan, H. Zreiqat, Short-term exposure to tumor necrosis factor- $\alpha$  enables human osteoblasts to direct adipose tissue-derived mesenchymal stem cells into osteogenic differentiation. *Stem Cells Dev.* **21**(13), 2420–2429 (2012)
96. S.C. Manolagas, Birth and death of bone cells: basic regulatory mechanisms and implications for the pathogenesis and treatment of osteoporosis. *Endocr. Rev.* **21**(2), 115–137 (2000)
97. A. Marathe, M.C. Peterson, D.E. Mager, Integrated cellular bone homeostasis model for denosumab pharmacodynamics in multiple myeloma patients. *J. Pharmacol. Exp. Ther.* **326**(2), 555–562 (2008). ISSN 1521-0103
98. T.J. Martin, E. Seeman, New mechanisms and targets in the treatment of bone fragility. *Clin. Sci.* **112**(2), 77–91 (2007). ISSN 1470-8736
99. M.R. McClung, A. Grauer, S. Boonen, M.A. Bolognese, J.P. Brown, A. Diez-Perez, B.L. Langdahl, J.-Y. Reginster, J.R. Zanchetta, S.M. Wasserman, L. Katz, J. Maddox, Y.-C. Yang, C. Libanati, H.G. Bone, Romosozumab in postmenopausal women with low bone mineral density. *N. Engl. J. Med.* **370**(5), 412–420 (2014). ISSN 0028-4793
100. B. Meibohm, H. Derendorf, Basic concepts of pharmacokinetic/pharmacodynamic (PK/PD) modelling. *Int. J. Clin. Pharmacol. Ther.* **35**(10), 401–13 (1997)
101. H. Michael, P.L. Hrknen, H.K. Vninen, T.A. Hentunen, Estrogen and testosterone use different cellular pathways to inhibit osteoclastogenesis and bone resorption. *J. Bone Mineral Res.* **20**(12), 2224–2232 (2005)
102. P.D. Miller, M.A. Bolognese, E.M. Lewiecki, M.R. McClung, B. Ding, M. Austin, Y. Liu, J. San Martin, Effect of denosumab on bone density and turnover in postmenopausal women with low bone mass after long-term continued, discontinued, and restarting of therapy: a randomized blinded phase 2 clinical trial. *Bone* **43**(2), 222–229 (2008). ISSN 8756-3282
103. R. Müller, Hierarchical microimaging of bone structure and function. *Nat. Rev. Rheumatol.* **5**(7), 373–381 (2009). ISSN 1759-4790
104. G.R. Mundy, Cellular and molecular regulation of bone turnover. *Bone* **24**(5 Suppl), 35S–38S (1999). ISSN 8756-3282
105. M.H. Murad, M.T. Drake, R.J. Mullan, K.F. Mauck, L.M. Stuart, M.A. Lane, N.O. Abu Elnour, P.J. Erwin, A. Hazem, M.A. Puhon, T. Li, V.M. Montori, Comparative effectiveness of drug treatments to prevent fragility fractures: a systematic review and network meta-analysis. *J. Clin. Endocrinol. Metab.* **97**(6), 1871–1880 (2012). ISSN 19457197
106. J.D. Murray, *Mathematical Biology: I. An Introduction*, vol. 1, 3rd edn. (Springer, New York, 2002)
107. N. Nakagawa, M. Kinosaki, K. Yamaguchi, N. Shima, H. Yasuda, K. Yano, T. Morinaga, K. Higashio, RANK is the essential signaling receptor for osteoclast differentiation factor in osteoclastogenesis. *Biochem. Biophys. Res. Commun.* **253**(2), 395–400 (1998)
108. T. Nakashima, M. Hayashi, T. Fukunaga, K. Kurata, M. Oh-hora, J.Q. Feng, L.F. Bonewald, T. Kodama, A. Wutz, E.F. Wagner, J.M. Penninger, H. Takayanagi, Evidence for osteocyte regulation of bone homeostasis through RANKL expression. *Nat. Med.* **17**(10), 1231–1234 (2011). ISSN 1078-8956
109. A. Nazarian, B.D. Snyder, D. Zurakowski, R. Müller, Quantitative micro-computed tomography: A non-invasive method to assess equivalent bone mineral density. *Bone* **43**(2), 302–311 (2008). ISSN 87563282
110. R.M. Neer, C.D. Arnaud, J.R. Zanchetta, R. Prince, G.A. Gaich, J.Y. Reginster, A.B. Hodsmann, E.F. Eriksen, S. Ish-Shalom, H.K. Genant, O. Wang, B.H. Mitlak, Effect of parathyroid hormone (1–34) on fractures and bone mineral density in postmenopausal women with osteoporosis. *N. Engl. J. Med.* **344**(19), 1434–1441 (2001). ISSN 0028-4793
111. M. Nilsson, C. Ohlsson, A. Odn, D. Mellström, M. Lorentzon, Increased physical activity is associated with enhanced development of peak bone mass in men: a five-year longitudinal study. *J. Bone Mineral Res.* **27**(5), 1206–1214 (2012). ISSN 1523-4681

112. S. Nuzzo, M.H. Lafage-Proust, R. Martin-Badosa, G. Boivin, T. Thomas, C. Alexandre, F. Peyrin, Synchrotron radiation microtomography allows the analysis of three-dimensional microarchitecture and degree of mineralization of human iliac crest biopsy specimens: effects of etidronate treatment. *J. Bone Mineral Res.* **17**(8), 1372–1382 (2002)
113. J.S. Nyman, A. Roy, X. Shen, R.L. Acuna, J.H. Tyler, X. Wang, The influence of water removal on the strength and toughness of cortical bone. *J. Biomech.* **39**(5), 931–938 (2006). ISSN 0021-9290
114. E. Ozcivici, Y.K. Luu, B. Adler, Y.-X. Qin, J. Rubin, S. Judex, C.T. Rubin, Mechanical signals as anabolic agents in bone. *Nat. Rev. Rheumatol.* **6**(1), 50–59 (2010). ISSN 1759-4790
115. D. Padhi, M. Allison, A.J. Kivitz, M.J. Gutierrez, B. Stouch, C. Wang, G. Jang, Multiple doses of sclerostin antibody romosozumab in healthy men and postmenopausal women with low bone mass: a randomized, double-blind, placebo-controlled study. *J. Clin. Pharmacol.* **54**(2), 168–178 (2014). ISSN 1552-4604
116. A.M. Parfitt, The physiological and clinical significance of bone histomorphometric data, *Bone Histomorphometry: Techniques and Interpretation* (CRC Press, Boca Raton, 1983)
117. A.M. Parfitt, *Calcium Homeostasis*, vol. 107 (Springer, Heidelberg, 1993), pp. 1–65
118. A.M. Parfitt, Osteonal and hemi-osteonal remodeling: the spatial and temporal framework for signal traffic in adult human bone. *J. Cell. Biochem.* **55**(3), 273–86 (1994). ISSN 0730-2312
119. M.C. Peterson, M.M. Riggs, A physiologically based mathematical model of integrated calcium homeostasis and bone remodeling. *Bone* **46**(1), 49–63 (2010). ISSN 1873-2763
120. P. Pivonka, S.V. Komarova, Mathematical modeling in bone biology: from intracellular signaling to tissue mechanics. *Bone* **47**(2), 181–189 (2010). ISSN 1873-2763
121. P. Pivonka, J. Zimak, D.W. Smith, B.S. Gardiner, C.R. Dunstan, N.A. Sims, T.J. Martin, G.R. Mundy, Model structure and control of bone remodeling: a theoretical study. *Bone* **43**(2), 249–263 (2008)
122. P. Pivonka, J. Zimak, D.W. Smith, B.S. Gardiner, C.R. Dunstan, N.A. Sims, T.J. Martin, G.R. Mundy, Theoretical investigation of the role of the RANK-RANKL-OPG system in bone remodeling. *J. Theor. Biol.* **262**(2), 306–316 (2010)
123. P. Pivonka, P.R. Buenzli, C.R. Dunstan, A systems approach to understanding bone cell interactions in health and disease, in *Cell Interact.*, ed. by S. Gowder (chapter 7) (InTech, 2012), pp. 169–204
124. T.M. Post, J.I. Freijer, J. DeJongh, M. Danhof, Disease system analysis: basic disease progression models in degenerative disease. *Pharm. Res.* **22**(7), 1038–1049 (2005). ISSN 07248741
125. T.M. Post, S.C.L.M. Cremers, T. Kerbusch, M. Danhof, Bone physiology, disease and treatment. *Clin. Pharmacokinet.* **49**(2), 89–118 (2010). ISSN 0312-5963
126. T.M. Post, S. Schmidt, L.A. Peletier, R. de Greef, T. Kerbusch, M. Danhof, Application of a mechanism-based disease systems model for osteoporosis to clinical data. *J. Pharmacokinet. Pharmacodyn.* **40**(2), 143–56 (2013). ISSN 1573-8744
127. S. Qiu, D.S. Rao, S. Palnitkar, A.M. Parfitt, Reduced iliac cancellous osteocyte density in patients with osteoporotic vertebral fracture. *J. Bone Mineral Res.* **18**(9), 1657–1663 (2003)
128. R.R. Recker, J. Lappe, K.M. Davies, R. Heaney, Remodeling increases substantially in the years after menopause and remains increased in older osteoporosis patients. *J. Bone Mineral Res.* **19**(10), 1628–1633 (2004)
129. J.-Y. Rho, L. Kuhn-Spearing, P. Zioupos, Mechanical properties and the hierarchical structure of bone. *Med. Eng. Phys.* **20**(2), 92–102 (1998). ISSN 1350-4533
130. B.L. Riggs, Overview of osteoporosis. *West. J. Med.* **154**(1), 63–77 (1991)
131. B.L. Riggs, A.M. Parfitt, Drugs used to treat osteoporosis: the critical need for a uniform nomenclature based on their action on bone remodeling. *J. Bone Mineral Res.* **20**(2), 177–184 (2005). ISSN 0884-0431
132. B.L. Riggs, H.W. Wahner, L.J. Melton, L.S. Richelson, H.L. Judd, K.P. Offord, *J. Clin. Invest.* **77**(5), 1487–1491 (1986). ISSN 00219738
133. B.L. Riggs, S. Khosla, L.J. Melton, A unitary model for involutional osteoporosis: estrogen deficiency causes both type I and type II osteoporosis in postmenopausal women and contributes to bone loss in aging men. *J. Bone Mineral Res.* **13**(5), 763–773 (1998). ISSN 0884-0431

134. R.O. Ritchie, The conflicts between strength and toughness. *Nat. Mater.* **10**(11), 817–22 (2011). ISSN 14761122
135. A.G. Robling, S.D. Stout, Morphology of the drifting osteon. *Cells Tissues Organs* **164**, 192–204 (1998)
136. G. Rodan, T.J. Martin, Role of osteoblasts in hormonal control of bone resorption a hypothesis. *Calcif. Tissue Int.* **33**(1), 349–351 (1981)
137. P. Roschger, S. Rinnerthaler, J. Yates, G.A. Rodan, P. Fratzl, K. Klaushofer, Alendronate increases degree and uniformity of mineralization in cancellous bone and decreases the porosity in cortical bone of osteoporotic women. *Bone* **29**(2), 185–191 (2001)
138. P. Roschger, H.S. Gupta, A. Berzlanovich, G. Ittner, D.W. Dempster, P. Fratzl, F. Cosman, M. Parisien, R. Lindsay, J.W. Nieves, K. Klaushofer, Constant mineralization density distribution in cancellous human bone. *Bone* **32**(3), 316–323 (2003)
139. P. Roschger, E.P. Paschalis, P. Fratzl, K. Klaushofer, Bone mineralization density distribution in health and disease. *Bone* **42**(3), 456–466 (2008)
140. D. Ruffoni, P. Fratzl, P. Roschger, K. Klaushofer, R. Weinkamer, The bone mineralization density distribution as a fingerprint of the mineralization process. *Bone* **40**(5), 1308–1319 (2007)
141. D. Ruffoni, P. Fratzl, P. Roschger, R. Phipps, K. Klaushofer, R. Weinkamer, Effect of temporal changes in bone turnover on the bone mineralization density distribution: a computer simulation study. *J. Bone Mineral Res.* **23**(12), 1905–1914 (2008)
142. M. Sadatsafavi, A. Moayyeri, L. Wang, and W. D. Leslie. Heteroscedastic regression analysis of factors affecting bmd monitoring. *Journal of Bone and Mineral Research*, **23** (11): 1842–1849, 2008. ISSN 1523-4681
143. P. Sambrook, C. Cooper, Osteoporosis. *Lancet* **367**, 2010–2018 (2006)
144. V. Sansalone, V. Bousson, S. Naili, C. Bergot, F. Peyrin, J.D. Laredo, G. Haiat, Anatomical distribution of the degree of mineralization of bone tissue in human femoral neck: impact on biomechanical properties. *Bone* **50**(4), 876–884 (2012)
145. S. Scheiner, P. Pivonka, C. Hellmich, Coupling systems biology with multiscale mechanics, for computer simulations of bone remodeling. *Comput. Methods Appl. Mech. Eng.* **254**(1), 181–196 (2013). ISSN 00457825
146. S. Scheiner, P. Pivonka, D.W. Smith, C.R. Dunstan, C. Hellmich, Mathematical modeling of postmenopausal osteoporosis and its treatment by the anti-catabolic drug denosumab. *Int. J. Numer. Method Biomed. Eng.* **30**(1), 1–27 (2014). ISSN 2040-7947
147. S. Schmidt, T.M. Post, L.A. Peletier, M.A. Boroujerdi, M. Danhof, Coping with time scales in disease systems analysis: application to bone remodeling. *J. Pharmacokinet. Pharmacodyn.* **38**(6), 873–900 (2011). ISSN 1567567X
148. A.V. Schwartz, D.C. Bauer, S.R. Cummings, J.A. Cauley, K.E. Ensrud, L. Palermo, R.B. Wallace, M.C. Hochberg, A.C. Feldstein, A. Lombardi, D.M. Black, Efficacy of continued alendronate for fractures in women with and without prevalent vertebral fracture: the FLEX trial. *J. Bone Mineral Res.* **25**(5), 976–982 (2010). ISSN 08840431
149. E. Seeman, Is a change in bone mineral density a sensitive and specific surrogate of anti-fracture efficacy? *Bone* **41**(3), 308–317 (2007). ISSN 8756-3282
150. E. Seeman, P.D. Delmas, Bone quality – the material and structural basis of bone strength and fragility. *N. Engl. J. Med.* **354**(21), 2250–2261 (2006). ISSN 1533-4406
151. M.J. Seibel, Biochemical markers of bone turnover – Part I: biochemistry and variability. *Clin. Biochem. Rev.* **26**(4), 97–122 (2005). ISSN 0159-8090
152. M.J. Seibel, Biochemical markers of bone turnover Part II: clinical applications in the management of osteoporosis. *Clin. Biochem. Rev.* **27**(3), 123–138 (2006). ISSN 0159-8090
153. E. Shane, D. Burr, P.R. Ebeling, B. Abrahamsen, R.A. Adler, T.D. Brown, A.M. Cheung, F. Cosman, J.R. Curtis, R. Dell, D. Dempster, T.A. Einhorn, H.K. Genant, P. Geusens, K. Klaushofer, K. Koval, J.M. Lane, F. McKiernan, R. McKinney, A. Ng, J. Nieves, R. O’Keefe, S. Papapoulos, H.T. Sen, M.C.H. van der Meulen, R.S. Weinstein, M. Whyte. Atypical subtrochanteric and diaphyseal femoral fractures: Report of a task force of the american society for bone and mineral research. *J. Bone Mineral Res.* **25**(11), 2267–2294 (2010). ISSN 1523-4681

154. L. Shargel, S. Wu-Pong, A.B.C. Yu, *Applied Biopharmaceutics & Pharmacokinetics*, 5th edn. (McGraw-Hill, New York, 2004) (Medical)
155. J.A. Shepherd, Y. Lu, K. Wilson, T. Fuerst, H. Genant, T.N. Hangartner, C. Wilson, D. Hans, E.S. Leib. Cross-calibration and minimum precision standards for Dual-Energy X-ray absorptiometry: the 2005 ISCD official positions. *J. Clin. Densitom.* **9**(1), 31–36 (2006). ISSN 1094-6950
156. H. Sievänen, P. Kannus, T.L.N. Järvinen, Bone quality: an empty term. *PLoS Med.* **4**(3), e27 (2007)
157. W.S. Simonet, D.L. Lacey, C.R. Dunstan, M. Kelley, M.S. Chang, R. Lüthy, H.Q. Nguyen, S. Wooden, L. Bennett, T. Boone, G. Shimamoto, M. DeRose, R. Elliott, A. Colombero, H.L. Tan, G. Trail, J. Sullivan, E. Davy, N. Bucay, L. Renshaw-Gegg, T.M. Hughes, D. Hill, W. Pattison, P. Campbell, S. Sander, G. Van, J. Tarpley, P. Derby, R. Lee, W.J. Boyle, Osteoprotegerin: a novel secreted protein involved in the regulation of bone density. *Cell* **89**(2), 309–319 (1997)
158. R.E. Small, Uses and limitations of bone mineral density measurements in the management of osteoporosis. *Medscape General Med.* **7**(2), 3–29 (2005). ISSN 1531-0132
159. T.H. Smit, E.H. Burger, Is BMU-coupling a strain-regulated phenomenon? A finite element analysis. *J. Bone Mineral Res.* **15**(2), 301–307 (2000)
160. T.H. Smit, E.H. Burger, J.M. Huyghe, A case for strain-induced fluid flow as a regulator of bmu-coupling and osteonal alignment. *J. Bone Mineral Res.* **17**(11), 2021–2029 (2002)
161. L.J. Smith, J.P. Schirer, N.L. Fazzalari, Bone mineralization density distribution in health and disease. *J. Biomech.* **43**(16), 3144–3149 (2010)
162. K.L. Stone, D.G. Seeley, L.-Y. Lui, J.A. Cauley, K. Ensrud, W.S. Browner, M.C. Nevitt, S.R. Cummings, BMD at multiple sites and risk of fracture of multiple types: long-term results from the study of osteoporotic fractures. *J. Bone Mineral Res.* **18**(11), 1947–1954 (2003). ISSN 1523-4681
163. P. Sutton-Smith, H. Beard, N. Fazzalari, Quantitative backscattered electron imaging of bone in proximal femur fragility fracture and medical illness. *J. Microsc.* **229**(Pt 1), 60–66 (2007)
164. P. Szulc, E. Seeman, Thinking inside and outside the envelopes of bone. *Osteoporos. Int.* **20**(8), 1281–1288 (2009). ISSN 1433-2965
165. S.L. Teitelbaum, F.P. Ross, Genetic regulation of osteoclast development and function. *Nat. Rev. Genet.* **4**(8), 638–649 (2003). ISSN 1471-0056
166. A.Y.-T. Teng, H. Nguyen, X. Gao, Y.-Y. Kong, R.M. Gorczynski, B. Singh, R.P. Ellen, J.M. Penninger, Functional human T-cell immunity and osteoprotegerin ligand control alveolar bone destruction in periodontal infection. *J. Clin. Invest.* **106**(6), R59–R67 (2000)
167. C.D.L. Thomas, S.A. Feik, J.G. Clement, Increase in pore area, and not pore density, is the main determinant in the development of porosity in human cortical bone. *J. Anat.* **209**, 219–230 (2006)
168. E. Tsuda, M. Goto, S. Mochizuki, K. Yano, F. Kobayashi, T. Morinaga, K. Higashio, Isolation of a novel cytokine from human fibroblasts that specifically inhibits osteoclastogenesis. *Biochem. Biophys. Res. Commun.* **234**(1), 137–142 (1997)
169. S.S.J. Webster, Integrated bone tissue physiology: anatomy and physiology, *Bone Mechanics Handbook*, 2nd edn. (CRC Press, Boca Raton, 2001)
170. S. Weiner, H.D. Wagner, The material bone: structure-mechanical function relations. *Annu. Rev. Mater. Sci.* **28**(8), 271–298 (1998)
171. R.S. Weinstein, True strength. *J. Bone Mineral Res.* **15**(4), 621–625 (2000). ISSN 1523-4681
172. M.N. Weitzmann, R. Pacifici, Estrogen deficiency and bone loss: an inflammatory tale. *J. Clin. Investig.* **116**(5), 1186–1194 (2006)
173. WHO: Assessment of fracture risk and its application to screening for postmenopausal osteoporosis. *World Health Organ. Techn. Rep. Ser.* **843** (1994)
174. WHO: Prevention and management of osteoporosis. *World Health Organ. Techn. Rep. Ser.* **921**, 1–164 (2003). ISSN 0512-3054
175. J.C. Wong, M.R. Griffiths, Precision of bone densitometry measurements: when is change true change and does it vary across bone density values? *Australas. Radiol.* **47**(3), 236–239 (2003)

176. H. Yasuda, N. Shima, N. Nakagawa, K. Yamaguchi, M. Kinosaki, S. Mochizuki, A. Tomoyasu, K. Yano, M. Goto, A. Murakami, E. Tsuda, T. Morinaga, K. Higashio, N. Udagawa, N. Takahashi, T. Suda, Osteoclast differentiation factor is a ligand for osteoprotegerin/osteoclastogenesis-inhibitory factor and is identical to TRANCE/RANKL. *Proc. Natl. Acad. Sci. USA* **95**(7), 3597–602 (1998). ISSN 0027-8424
177. E.A. Zimmermann, B. Busse, R.O. Ritchie, The fracture mechanics of human bone: influence of disease and treatment. *BoneKEy Rep.* **4**(September), 743 (2015). ISSN 2047-6396
178. P.K. Zysset, E. Dall'Ara, P. Varga, D.H. Pahr, Finite element analysis for prediction of bone strength. *BoneKEy Rep.* **2**(386), e1–e9 (2013). ISSN 2047-6396

Multiscale Mechanobiology of Bone Remodeling and  
Adaptation

Pivonka, P. (Ed.)

2018, XII, 287 p. 98 illus., Hardcover

ISBN: 978-3-319-58843-8